smaller and limited than that under eccentric contraction, it is also known that gene expression response is produced under concentric muscle contraction. Chan et al. (2004) studied cytokine gene expression in human skeletal muscle after concentric contraction and showed that IL-6 and IL-8 mRNA expressions significantly increased [7]. Most recently, Mckenzie and Goldfarb (2007) evaluated the gene transcription in rat soleus after aerobic exercise (running on the treadmill for 2 h) using microarray technique and identified that 52 genes significantly altered by the exercise [8]. In their report, the major gene families altered were metabolism, apoptosis, muscle contraction, transcription/cell signaling, tissue generation, and inflammation.

Based on above studies, dramatic molecular responses of masticatory muscles would be predicted during and after contraction. However, since it is known that the anatomical characteristics (e.g., fiber type, diameter) of jaw-closing muscle fibers are different from those of limb and abdominal muscles [9–12], masticatory muscles would be expected to have a wider repertoire of contractile protein expression and function [13]. These anatomical differences lead us to suspect that the biological characteristics of masticatory muscles may also be different from those of the limb muscles. In order to clarify the molecular responses of masticatory muscle to contraction, a specific experiment is needed. We purposed to evaluate the comprehensive gene expression profile changes induced in the mouse masseter muscle tissue after repetitive electrical stimulation, by using a cDNA microarray technique.

2. Materials and methods

2.1. Animals

Nine male ICR mice aged 10 weeks were used in this study. Under general anesthesia (urethane:pentobarbital = 1:1, 0.14 ml/100 g) by intraperitoneal injection, each mouse was set on a platform in a supine position and the upper incisors were secured to the platform. One centimeter skin cut was performed on both cheek region to expose the masseter muscle proper. Bipolar electrodes were set on the right masseteric fascia to electrically stimulate the masseter muscle (8 V, 10 Hz, 20 ms) for 30 min. The left side masseter muscle was kept exposed for 30 min but was not stimulated. To confirm the repetitive muscle contraction was induced, both masseter muscles were observed visually during the experiment. To prevent drying of the muscle tissues, mineral oil (SIGMA, St. Louis, MO, USA) was dropped over both masseter muscles during the electrical stimulation period. After cessation of the stimulation, each mouse was kept on the platform and bilateral masseter muscle tissues were sampled 0 h ($n = 3$), 1 h ($n = 3$) and 2 h ($n = 3$). The obtained muscle tissues were immediately frozen by liquid nitrogen for later RNA isolation. The experimental protocol of this study was reviewed and approved by the animal research control committee of Okayama University Graduate School of Medicine, Dentistry and Pharmaceutical Sciences (#OKU-2006188).

2.2. RNA extraction and probe preparation

Masseter muscle total RNA was isolated from each individual sample with TRI_{ZOL} Reagent® (Invitrogen, Carlsbad, CA, USA) according to the manufacture's instructions and pooled group-wise for analysis. Muscle samples weighing approximately 50 mg each were homogenized in 1 mL of TRI_{ZOL}. Following chloroform extraction, RNA was precipitated with isopropyl alcohol and washed with 70% ethanol. The purity and concentration of RNA were determined by measurement of absorbance at 260 and 280 nm.

Total RNA samples (35 μg) were labeled with Cy3-dCTP (as stimulation side) or Cy5-dCTP (as control side) using the Cyscribe First-Strand cDNA Labelling Kit (Amercham Biosciences, Amersham Place Little Chalfont Buckinghamshire, England) according to the manufacture's instructions.

2.3. Microarray hybridization and signal detection

Fluorescently labeled samples were processed and hybridized with cDNA microarray slide (Mouse 6.4 k oligo DNA Microarray, Nippon Laser & Electronics Lab, Nagoya, Japan), which is aminosilane-coated slide-glass, contains the 6400 marker genes representing 12 important functional classifications: (1) apoptosis, (2) stem cell, (3) neuroscience, (4) developmental/regenerative disease, (5) cancer, (6) diabetes/obesity, (7) cell cycle, (8) extracellular matrix and adhesion molecules, (9) autoimmune/inflammatory disease, (10) toxicology and drug metabolism, (11) cardiovascular disease, and (12) signal transduction. Hybridization procedure was performed using UltraGAPS Coated Slides (Corning, Lowell, MA, USA) according to the manufacture's instructions, then poly(A)RNAλ (TAKARA, Otsu, Japan) was mixed with labeled samples as the spiking controls. The hybridized slides were scanned with GenePix 4000B (Molecular Devices, Sunnyvale, CA, USA) using appropriate gains on the photomultiplier tube (PMT) to obtain the highest intensity without saturation. TIFF image was generated for each channel, Cy3 and Cy5. The signal intensity was transformed to numerical value with the Array Vision (IMAGING Research Inc., Ontario, Canada).

2.4. Data analysis

Probe arrays were then scanned and analyzed to calculate the signal density using the computer software (Mouse DNA Chip Consortium ver.1, INTEC Web and Genome Informatics Corporation, Tokyo, Japan). Spots with background-subtracted intensity, which were lower than 0 in either Cy3 or Cy5 channel were filtered out. Global normalization was then applied to correct the artifacts caused by different dye incorporation rates or scanner settings for two dyes. Additionally, the digital signals were normalized with the Lowess algorithm (0.33). Gene expression profiles were compared at each time point between the right (stimulation side) and left (control side) masseter. The ratio of each side gene expression (right/left) was indicated as a logarithm in the data table. When the gene

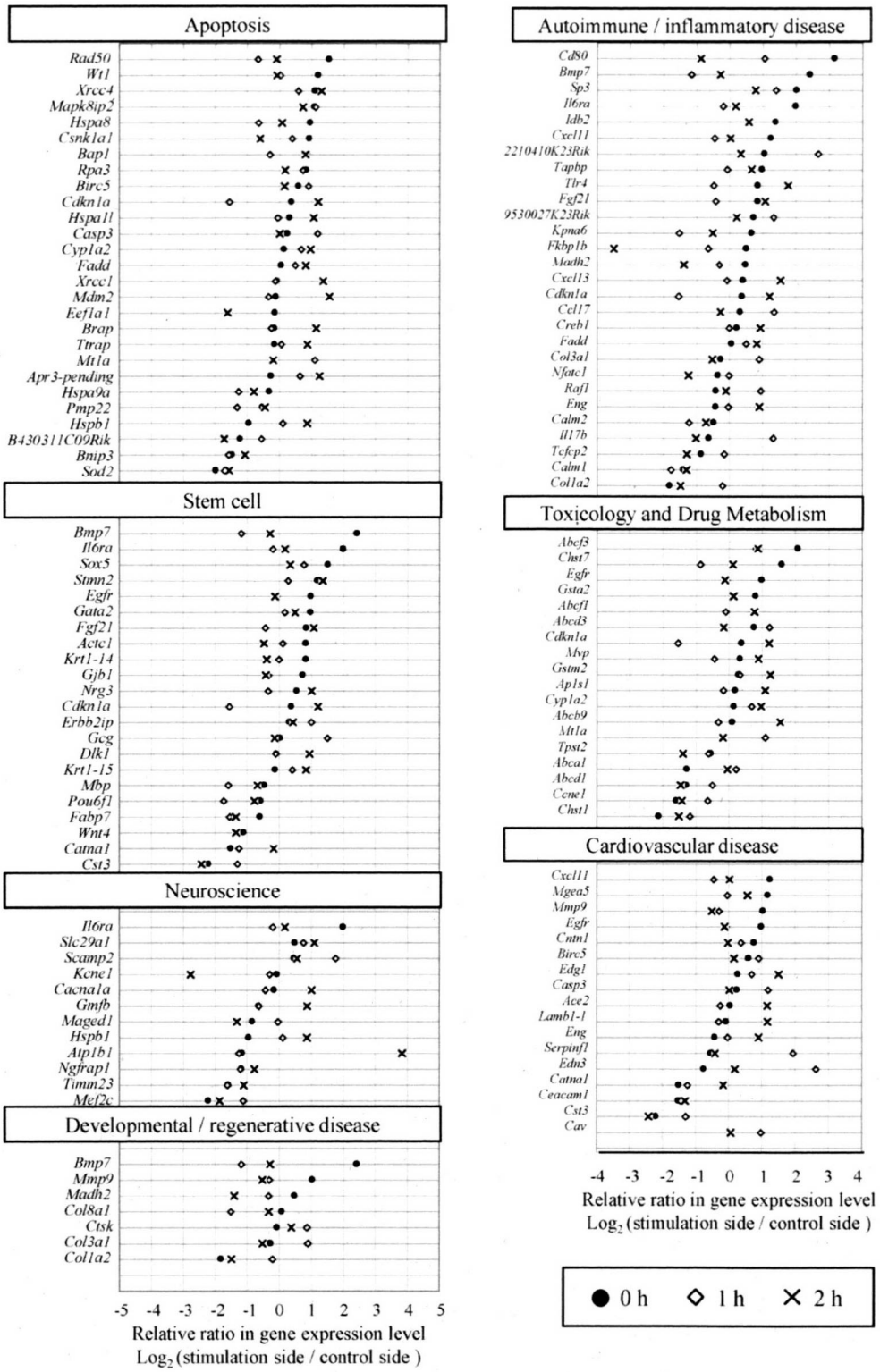

Fig. 1. Functional classification of muscle genes that showed a more than 2-fold change in expression level by electrical stimulation or not. The horizontal axis shows fold of changes (log 2) at each time point. Functional classification of muscle genes was based on the annotation system (Mouse DNA Chip Consortium ver.1, INTEC Web and Genome Informatics Corporation, Tokyo, Japan).

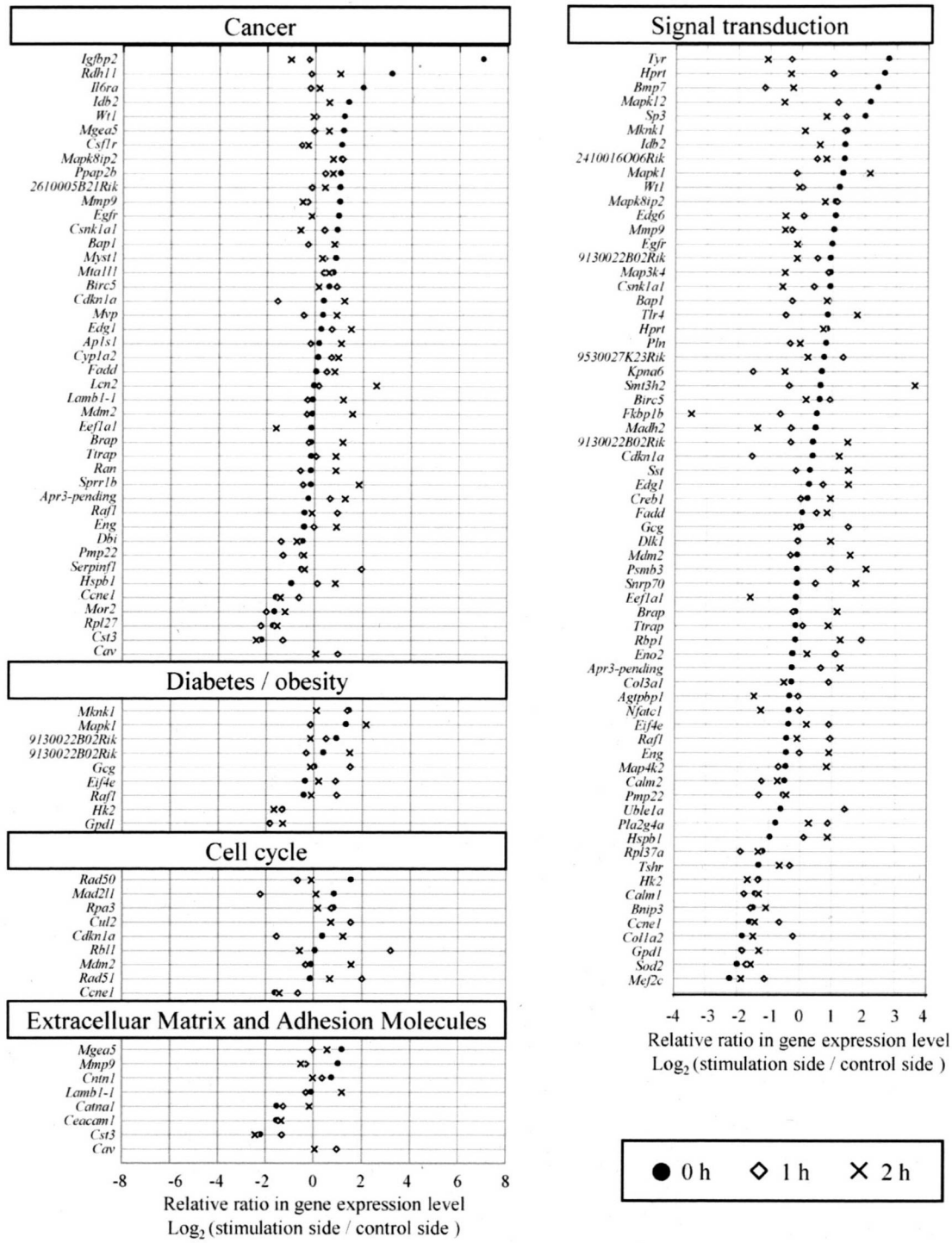

Fig. 1. (*Continued*).

expression levels were different more than 2-fold ($\log 2 \geq 1$: up-regulated or $\log 2 \leq -1$: down-regulated), the difference was regarded positive [14].

3. Results

Of the 6400 genes assessed, 1733 genes were up-regulated and 515 genes were down-regulated from the stimulation side at least once during the experimental time points. 28 genes were up-regulated and 25 genes were down-regulated at all time points. However, those 53 genes could not be classified into any functional categories, because they all were not listed in the gene annotation database (FANTOM II, GenBank and UniGene). The genes which showed positive differences between right and left masseter at each time point are shown in Fig. 1 in each functional category. As shown in Fig. 1, the up-

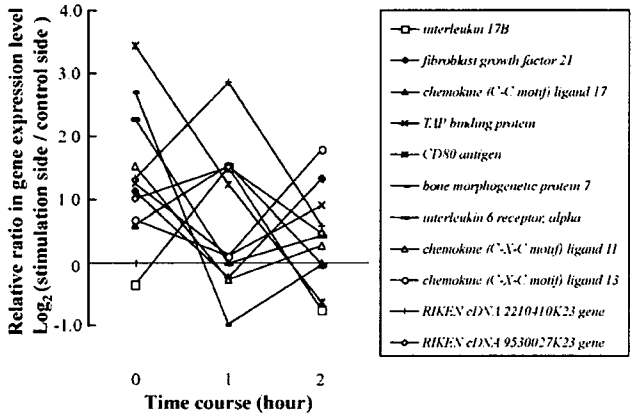

Fig. 2. Changes of muscle genes related to "cytokine and inflammatory response" which indicated a more than 2-fold changes ($\log 2 \geq 1$ or $\log 2 \leq -1$) in expression levels at least once during the experimental time course.

or down-regulated genes at least once during the experimental time course were associated with autoimmune/inflammatory disease (28/114), cardiovascular disease (17/61), neuroscience (12/50), apoptosis (27/93), diabetes/obesity (9/28) and signal transduction (66/250) and others.

Since previous studies provided the data to support the notion that several kinds of cytokines play important role for muscle metabolism changes related to muscle contraction [7,15–20], the data on 'cytokine and inflammatory response' were also analyzed in detail. As a result, 11 genes in relation to 'cytokine and inflammatory response' were up-regulated at least once during the three time points in this study (Fig. 2). In particular, marked expression changes were observed in CD80 antigen, bone morphogenetic protein 7, interleukin 6 receptor alpha, and RIKEN cDNA 2210410K23 gene during the experimental time course. The expression levels of these genes were over 4-fold when compared with those in not stimulated contralateral side.

4. Discussion

In order to improve our understanding of the molecular events underlying masticatory muscle contraction, mRNA expression profiling in mouse masseter after repetitive muscle contraction was performed. In this study, concurrent measurement of the magnitude of masseter contraction during electrical stimulation was not elected since EMG needle electrodes could induce local inflammation in muscle proper. However, we did insert the needle electrode into the masseter muscle tissue in our pilot study using several mice to confirm proper muscle activity was consistently induced by the level of electrical stimulation used in this experiment. Additionally, repetitive muscle contractions were certainly confirmed visually during the experiments. For these reasons, it is considered that our electrical stimulation method used in this study actually induced masseter muscle activity.

Overall a fairly dramatic molecular response in mouse masseter muscles were observed and of the 6400 genes assessed, 1733 genes were up-regulated and 515 genes were down-regulated on the stimulation side at least once during the experimental time points. This data does not allow us to determine the functional meaning of these gene expression changes at this stage. Also, the mRNA expression levels of cytokines were carefully analyzed, because it is known that the several cytokines play important role for muscle metabolism changes related to muscle contraction [7,15–21]. Several kinds of cytokine mRNA levels changed after the cessation of the electrical stimulation. Previous study demonstrated that IL-6 gene expression levels significantly increased after cessation of the repetitive contraction using rat masseter muscle [21]. Other research findings also suggested that up-regulation of IL-6 and IL-6 receptor gene expression in muscle tissues can be a good marker of muscle contraction [15,17–23]. Therefore, we paid attention to the IL-6 receptor alpha gene levels. Since the up-regulation of IL-6 receptor alpha gene was certainly observed, these results suggest the excellent validity of this experimental muscle contraction model. Regarding the function of IL-6 produced in contracting muscle tissues, several reports suggest it may work as an energy sensor within the muscle cells [24]. Other organs also release IL-6 during exercise; however, muscle-derived IL-6 seems to play an important role in signaling between the muscles and other organs in order to maintain energy supply. Moreover, muscle-derived IL-6 is likely to initiate many of the exercise associated immune changes, as IL-6 can increase plasma levels of the cytokines IL-1 ra and IL-10, together with cortisol and blood neutrophils [19]. It is also known that IL-6 inhibits low-level TNF-α production [23], thus anti-inflammatory effect of IL-6 is widely speculated by numerous researchers.

Before closing the manuscript, we would like to mention the shortcomings of the study. Since the array slides utilized in this study could not measure the every gene which is known to express in skeletal muscle tissues, we need to recognize that there will be other genes that show larger expression changes by electrical stimulation. Additional research studies, which are under consideration of these matters, would be desirable.

In summary, the present study found that the dramatic gene expression changes were induced by the repetitive electrical muscle stimulation in mouse masseter using microarray technique. These data will provide useful information for the scientists whose research target is a further understanding of masticatory muscle biology. In addition to the mRNA expression levels analyzed in this study, evaluation of other gene expression levels, which were not involved on the microarray slide utilized in current study, is also needed. Furthermore, by using the assessment of protein production levels in masticatory muscles during and after muscle contraction is promising to get better understanding of the masticatory muscle biology.

5. Conclusions

Within the limitation of this study, the results suggested that the dramatic gene expression changes were induced by the repetitive electrical muscle stimulation in mouse masseter muscle.

Acknowledgements

This study was partially supported in part by grant-in-aids for scientific research from the Ministry of Education, Science, Sports, and Culture of Japan (for KM: #12671883, #18659572, and for TK: #13877327). A preliminary report was presented at the 82th General Session and Exhibition of the IADR, 3/12/2004, Hawaii, USA.

References

[1] Fricton JR, Kroening R, Haley D, Siegert R. Myofascial pain syndrome of the head and neck: a review of clinical characteristics of 164 patients. Oral Surg Oral Med Oral Pathol 1985;60:615–23.
[2] Bush FM, Whitehill JM, Martelli MF. Pain assessment in temporomandibular disorders. Cranio 1989;7:137–43.
[3] Dao TT, Lund JP, Lavigne GJ. Comparison of pain and quality of life in bruxers and patients with myofascial pain of the masticatory muscles. J Orofac Pain 1994;8:350–6.
[4] Glaros AG, Tabacchi KN, Glass EG. Effect of parafunctional clenching on TMD pain. J Orofac Pain 1998;12:145–52.
[5] van Selms MK, Lobbezoo F, Wicks DJ, Hamburger HL, Naeije M. Craniomandibular pain, oral parafunctions, and psychological stress in a longitudinal case study. J Oral Rehabil 2004;31:738–45.
[6] Chen YW, Hubal MJ, Hoffman EP, Thompson PD, Clarkson PM. Molecular responses of human muscle to eccentric exercise. J Appl Physiol 2003;95:2485–94.
[7] Chan MH, Carey AL, Watt MJ, Febbraio MA. Cytokine gene expression in human skeletal muscle during concentric contraction: evidence that IL-8, like IL-6, is influenced by glycogen availability. Am J Physiol Regul Integr Comp Physiol 2004;287:R322–7.
[8] Mckenzie MJ, Goldfarb AH. Aerobic exercise bout effects on gene transcription in the rat soleus. Med Sci Sports Exerc 2007;39:1515–21.
[9] Tuxen A, Kirkeby S. An animal model for human masseter muscle: histochemical characterization of mouse, rat, rabbit, cat, dog, pig, and cow masseter muscle. J Oral Maxillofac Surg 1990;48:1063–7.
[10] Rowlerson A, Mascarello F, Veggetti A, Carpene E. The fibre-type composition of the first branchial arch muscles in carnivora and primates. J Muscle Res Cell Motil 1983;4:443–72.
[11] Desaki J, Fujita H, Okumura N, Sakanaka M. Immuno-electron-microscopic localization of basic fibroblast growth factor in the dystrophic mdx mouse masseter muscle. Cell Tissue Res 1992;270:569–76.
[12] Muller J, Vayssiere N, Royuela M, Leger ME, Muller A, Bacou F, et al. Comparative evolution of muscular dystrophy in diaphragm, gastrocnemius and masseter muscles from old male mdx mice. J Muscle Res Cell Motil 2001;22:133–9.
[13] Sciote JJ, Horton MJ, Rowlerson AM, Link J. Specialized cranial muscles: how different are they from limb and abdominal muscles? Cells Tissues Organs 2003;174:73–86.
[14] Schena M, Shalon D, Heller R, Chai A, Brown PO, Davis RW. Parallel human genome analysis: microarray-based expression monitoring of 1000 genes. Proc Natl Acad Sci USA 1996;93:10614–9.
[15] Jonsdottir IH, Schjerling P, Ostrowski K, Asp S, Richter EA, Pedersen BK. Muscle contractions induce interleukin-6 mRNA production in rat skeletal muscles. J Physiol 2000;528:157–63.
[16] Sasaki F, Shindoh C, Niwa T, Ohtaka T, Shindoh Y. Effects of interleukin-18 on diaphragm muscle contraction on rats. Tohoku J Exp Med 2002;196:269–80.
[17] Steensberg A, Keller C, Starkie RL, Osada T, Febbraio MA, Pedersen BK. IL-6 and TNF-alpha expression in, and release from, contracting human skeletal muscle. Am J Physiol Endocrinol Metab 2002;283:E1272–8.
[18] Pedersen BK, Steensberg A, Keller P, Keller C, Fischer C, Hiscock N, et al. Muscle-derived interleukin-6: lipolytic, anti-inflammatory and immune regulatory effects. Pflugers Arch 2003;446:9–16.
[19] Steensberg A. The role of IL-6 in exercise-induced immune changes and metabolism. Exerc Immunol Rev 2003;9:40–7.
[20] Rosendal L, Sogaard K, Kjaer M, Sjogaard G, Langberg H, Kristiansen J. Increase in interstitial interleukin-6 of human skeletal muscle with repetitive low-force exercise. J Appl Physiol 2005;98:477–81.
[21] Ono T, Maekawa K, Watanabe S, Oka H, Kuboki T. Muscle contraction accelerates IL-6 mRNA expression in the rat masseter muscle. Arch Oral Biol 2007;52:479–86.
[22] Keller C, Steensberg A, Hansen AK, Fischer CP, Plomgaard P, Pedersen BK. Effect of exercise, training, and glycogen availability on IL-6 receptor expression in human skeletal muscle. J Appl Physiol 2005;99:2075–9.
[23] Pedersen BK, Steensberg A, Fischer C, Keller C, Keller P, Plomgaard P, et al. The metabolic role of IL-6 produced during exercise: is IL-6 an exercise factor? Proc Nutr Soc 2004;63:263–7.
[24] Hoene M, Weigert C. The role of interleukin-6 in insulin resistance, body fat distribution and energy balance. Obes Rev 2008;9:20–9.

Neuroscience 159 (2009) 1422–1429

BOTULINUM TOXIN TYPE A (150 kDa) DECREASES EXAGGERATED NEUROTRANSMITTER RELEASE FROM TRIGEMINAL GANGLION NEURONS AND RELIEVES NEUROPATHY BEHAVIORS INDUCED BY INFRAORBITAL NERVE CONSTRICTION

Y. KITAMURA,[a] Y. MATSUKA,[a] I. SPIGELMAN,[b] Y. ISHIHARA,[c] Y. YAMAMOTO,[d] W. SONOYAMA,[a] T. KUBOKI[a]* AND K. OGUMA[d]

[a]*Department of Oral Rehabilitation and Regenerative Medicine, Okayama University Graduate School of Medicine, Dentistry and Pharmaceutical Sciences, 2-5-1 Shikata-cho, Okayama, 700–8525, Japan*

[b]*Division of Oral Biology and Medicine, School of Dentistry, University of California, 63-078 CHS, 10833 Le Conte Ave., Los Angeles, CA, 90095-1668, USA*

[c]*Department of Orthodontics and Dentofacial Orthopedics, Okayama University Graduate School of Medicine, Dentistry and Pharmaceutical Sciences, 2-5-1 Shikata-cho, Okayama, 700-8525, Japan*

[d]*Department of Bacteriology, Okayama University Graduate School of Medicine, Dentistry and Pharmaceutical Sciences, 2-5-1 Shikata-cho, Okayama, 700-8525, Japan*

Abstract—Many patients with trigeminal neuropathies suffer severe chronic pain which is inadequately alleviated with centrally-acting drugs. These drugs also possess severe side effects making compliance difficult. One strategy is to develop new treatments without central side effects by targeting peripheral sensory neurons, since sensory neuron excitability and neurotransmitter release increase in chronic pain states. Such treatments may include the highly purified botulinum toxin type A 150 kDa (BoNT/A) which reportedly blocks vesicular neurotransmitter release. We set out to determine if experimental trigeminal neuropathy induced by infraorbital nerve constriction (IoNC) in rats could alter neurotransmitter release from somata of trigeminal sensory neurons and if it could be attenuated by BoNT/A. Thus, we monitored the secretory activity of acutely dissociated trigeminal ganglion (TRG) neurons from naïve and IoNC rats by measuring the fluorescence intensity of the membrane-uptake marker (N-(3-triethylammoniumpropyl)-4-(6-(4-(diethylamino)phenyl)hexatrienyl)pyridinium dibromide (FM4-64). FM4-64 staining showed that neurons possess a pool of recycled vesicles which could be released by high KCl (75 mM) application. BoNT/A pre-treatment of acutely dissociated TRG neurons from naïve rats significantly reduced the rate of FM4-64 dye release. Neurons isolated from TRG ipsilateral to IoNC exhibited significantly faster onset of FM4-64 release than neurons contralateral to IoNC (sham surgery). IoNC also produced long-lasting ipsilateral tactile allodynia, measured as large decreases of withdrawal thresholds to mechanical stimulation. Intradermal injection of BoNT/A in the area of infraorbital branch of the trigeminal nerve (IoN) innervation alleviated IoNC-induced mechanical allodynia and reduced the exaggerated FM4-64 release in TRG neurons from these rats. Our results suggest that BoNT/A decreases neuropathic pain behaviors by decreasing the exaggerated neurotransmitter release from TRG sensory neurons.

Key words: botulinum toxin, neurotoxin, trigeminal ganglion, neurotransmitter release, somata, tactile allodynia.

Trigeminal neuralgia (TN) is one of the classic neuropathic pain disorders characterized by recurrent episodes of intense, lancinating pain felt in one or more divisions of the trigeminal distribution, either spontaneously or on gentle tactile stimulation of a trigger point on the face or in the oral cavity (Fromm, 1989; Rappaport and Devor, 1994). The treatment of TN continues to be a major therapeutic challenge. While the antiepileptic drug, carbamazepine, continues to be the treatment of choice (Zakrzewska and Patsalos, 1992; Li et al., 2004), a substantial proportion of patients tolerate this drug poorly because of central nervous system (CNS) side effects (e.g. dizziness, drowsiness). More effective and safer drugs are therefore required to treat debilitating neuropathic pain conditions such as TN.

Various rodent models of peripheral nerve injury have been developed which mimic human neuropathy symptoms of tactile allodynia, thermal hyperalgesia and spontaneous pain (Bennett and Xie, 1988; Kim and Chung, 1992; Seltzer et al., 1990; Mosconi and Kruger, 1996; Vos et al., 1994). It is now well established that the hyperexcitability of injured or neighboring primary sensory neurons is a major contributor to the development and maintenance of these neuropathy behaviors (reviewed in Gold, 2000; Devor, 2006; Dray, 2008). Neuropathic hyperexcitable afferents are also expected to exhibit increases in excitatory neurotransmitter release. Such increases in glutamate and neuropeptides have been demonstrated in the spinal dorsal horn of neuropathic rats (Skilling et al., 1992; Mark et al., 1998; Gardell et al., 2003; Coderre et al., 2005). Transmitter release is generally considered to occur at the peripheral and central terminals of primary sensory neurons. However, the somata of neurons in sensory ganglia were also demonstrated to be capable of transmitter release (Huang and Neher, 1996; Ulrich-Lai et al., 2001; Neubert

*Corresponding author. Tel: +81-86-235-6680; fax: +81-86-235-6684.
E-mail address: kuboki@md.okayama-u.ac.jp (T. Kuboki).

Abbreviations: BoNT, botulinum toxin; BoNT/A, botulinum toxin type A; CGRP, calcitonin gene-related peptide; CLS, confocal laser scanning; CNS, central nervous system; FBS, fetal bovine serum; FM4-64, (N-(3-triethylammoniumpropyl)-4-(6-(4-(diethylamino)phenyl)hexatrienyl)pyridinium dibromide; HBSS, Hanks' balanced salt solution; HWT, head withdrawal threshold; IB4, isolectin B4; IoN, infraorbital branch of the trigeminal nerve; IoNC, infraorbital nerve constriction; i.p., intraperitoneal; MEM, minimal essential medium; N-VGCC, N-type voltage-gated calcium channel; SNAP25, synaptosomal-associated protein, 25 kDa; SNARE, soluble *N*-ethylmaleimide sensitive factor attachment protein receptor; TN, trigeminal neuralgia; TRG, trigeminal ganglion; TTX, tetrodotoxin.

0306-4522/09 $ - see front matter
doi:10.1016/j.neuroscience.2009.01.066

et al., 2000; Matsuka et al., 2001). Additional evidence for a more active role of somata in sensory signal transmission, especially in pathological states, had come from the demonstrated increases in excitability of sensory neurons and the development of spontaneous ectopic discharge which originated within sensory ganglia after peripheral injury (Kirk, 1974; Kajander et al., 1992; Sheen and Chang, 1993; Xie et al., 1995; Zhang et al., 1997). After injury, neurons within sensory ganglia also exhibit potentiated cross-excitation among neighboring sensory neurons in the absence of synaptic specializations (Devor and Wall, 1990). Cross-excitation occurs when discharge in one sensory neuron leads to a depolarization in the cell bodies of adjacent passive neurons sharing the same ganglion. Cross-excitation was reported to be chemically mediated (Amir and Devor, 1996), but the identity of the chemical mediator(s) remains unknown. Both calcium-dependent and calcium-independent cross-excitation of vagal sensory neurons was also demonstrated (Oh and Weinreich, 2002).

A goal of our research is to develop new treatment methods that decrease chronic pain without severe central side effects. One strategy is to develop new treatments by targeting peripheral sensory neurons whose excitability and neurotransmitter release is increased in chronic pain states. Targeted treatments which do not penetrate the blood–brain-barrier should theoretically limit central side effects. One such treatment is botulinum toxin (BoNT), which reportedly blocks vesicular neurotransmitter release by disabling the soluble *N*-ethylmaleimide sensitive factor attachment protein receptor (SNARE) complex proteins which mediate vesicular transmitter release (Niemann et al., 1994; Schiavo et al., 2000). Indeed, clinicians have used BoNT, outside the product license, to treat chronic pain symptoms not associated with muscle spasms (Jeynes and Gauci, 2008). Previous studies demonstrated that BoNT is capable of attenuating release of substance P, calcitonin gene-related peptide (CGRP), or glutamate from sensory neurons in culture (Welch et al., 2000; Durham et al., 2004; Coderre et al., 2005; Meng et al., 2007), in isolated preparations (Ishikawa et al., 2000) and *in vivo* (Cui et al., 2004). These actions were proposed to contribute to the effectiveness of BoNT in attenuating pain symptoms of inflammation, migraine and neuropathies (Cui et al., 2004; Durham et al., 2004; Bach-Rojecky et al., 2005; Luvisetto et al., 2006, 2007; reviewed in Jeynes and Gauci, 2008). However, evidence linking neuropathy-induced increase in transmitter release from sensory neurons and its attenuation by BoNT as a plausible mechanism for attenuating pain of neuropathy has been lacking.

Here we report that unilateral infraorbital nerve constriction (IoNC) in rats produces long-lasting neuropathy behaviors which are concomitant with faster onset and increased magnitude of transmitter release from somata of trigeminal ganglion (TRG) neurons acutely isolated from the side of the injury. We also demonstrate that peripheral injection of botulinum toxin type A (BoNT/A) alleviates the IoNC-induced neuropathy behaviors and decreases the exaggerated neurotransmitter release in neurons acutely isolated from TRG ipsilateral to IoNC.

EXPERIMENTAL PROCEDURES

Trigeminal neuropathy model

All procedures regarding animal usage in this study were performed in accordance to specifications of an animal protocol approved by Okayama University (OKU-2007137). All experiments were conformed to relevant National Institutes of Health guidelines on the ethical use of animals. We minimized the number of animals used and their suffering. The unilateral constriction of the infraorbital branch of the trigeminal nerve (IoN) was made according to the method described by Vos et al. (1994). Adult male Sprague–Dawley rats (200–250 g) were anesthetized by intraperitoneal (i.p.) injection with ketamine (35 mg/kg) and xylazine (5 mg/kg), the IoN was exposed and two silk ligatures (4–0) were loosely tied around the IoN at about 2 mm apart. To obtain the desired degree of constriction a criterion formulated by Bennett and Xie (1988) was applied: the ligations reduced the diameter of the nerve by a just noticeable amount and retarded, but did not occlude the circulation through the superficial vasculature. The skin incision was closed in layers using nylon sutures (4–0). The contralateral side was subjected to sham surgery, where the IoN was exposed using the above procedures, but not constricted.

Sensory testing

On the day of sensory testing rat were lightly anesthetized (isoflurane) and their whiskers were shaved bilaterally to avoid their direct stimulation. After recovery from anesthesia mechanical sensitivity was assessed using the electronic "von Frey hair" pressure transducer (Model 1601C, IITC Instruments, Woodland Hills, CA, USA). Rats were placed in a fitted cloth restrainer (rat sling suit RSFC2, Lomir Biomedical, Malone, NY, USA) which was suspended 10 cm from the tabletop and allowed for unrestricted head movement during stimulation. Force was applied within the IoN territory of the snout at the center of the whisker pad (i.e. between rows B and C of the vibrissae) until the animal withdrew its head. Stimuli were alternated between the ipsilateral and contralateral sides, with 1 min recovery between iterations. Five iterations were averaged for each side. Baseline behavioral testing was performed one day before or same-day prior to the IoN surgery. On post-operative day 3, rats were anesthetized by i.p. injection with ketamine (35 mg/kg) and xylazine (5 mg/kg) for injections. Purified BoNT/A composed of a light and heavy chain (Lee et al., 2007) was administered as a single intradermal injection (100 pg in 0.1 ml of sterile saline) in the center of the whisker pad. All rats were injected intradermally with saline on the contralateral side and either saline or BoNT/A in saline on the ipsilateral side of the snout at the center of the whisker pad (i.e. between rows B and C of the vibrissae). The bleb of the injection materials was absorbed within a day. Sensory testing was repeated on post-operative day 14 (11 days after injection). Force was applied at the same point as during baseline testing.

Dissociation of TRG neurons

After sensory testing, animals were deeply anesthetized with ketamine (35 mg/kg) and xylazine (5 mg/kg i.p.). The TRG were harvested and cut into small pieces in ice-cold Hanks' balanced salt solution (HBSS, Sigma, St. Louis, MO, USA) supplemented with 20% fetal bovine serum (FBS, Bio Serum Co., Japan) and incubated for 30 min at 37 °C in 5 ml of minimal essential medium (MEM, GIBCO, Carlsbad, CA, USA) with 10% FBS, 2 mM glutamine, 24 mg/l insulin, 0.125% collagenase P (Roche, Indianapolis, IN, USA) and 0.02% DNase (Sigma). TRG were transferred for 5 min at 37 °C to 2 ml of Ca^{2+}– and Mg^{2+}–free HBSS (Sigma) containing 0.25% trypsin (Sigma) and 0.05% DNase. Cells were dissociated by tissue trituration with a series of fire-polished Pasteur pipettes in 5 ml HBSS containing 0.295% $MgSO_4$ and 0.02% DNase. Dissociated cells were suspended into MEM with 10% FBS and plated on 12 mm cover glass coated with poly-D-lysine

(Becton Dickinson, Franklin Lakes, NJ, USA) with 10 mm diameter cloning cylinder (Sigma). In some experiments, the cells were incubated with BoNT/A (10 ng in 60 μl of MEM). All experiments were performed within 1.5 h of tissue harvest.

FM4-64 dye staining, confocal imaging and analysis

Dissociated cells were tested with (N-(3-triethylammoniumpropyl)-4-(6-(4-(diethylamino)phenyl)hexatrienyl)pyridinium dibromide (FM4-64) dye (Molecular Probes, Eugene, OR, USA) 4–8 h after dissociation, as described previously (Matsuka et al., 2007). FM4-64 dye (10 μM) was added in control external solution (control solution) (mM) NaCl 119; KCl 5; glucose 30; Hepes 25; $CaCl_2$ 2; $MgCl_2$ 2 adjusted to pH 7.2 with NaOH and 310 mmol/kg osmolality, or in high KCl external solution (high K^+ solution) (mM) NaCl 49; KCl 75; glucose 30; Hepes 25; $CaCl_2$ 2; $MgCl_2$ 2 adjusted to pH 7.2 with NaOH and 310 mmol/kg osmolality. To load the dye, neurons were incubated in the high K^+ solution containing FM4-64 (10 μM) for 1 min. Cells were then washed three times with control solution to remove extracellular FM4-64. For vesicular release experiments, neurons were stimulated with the high K^+ solution without the FM4-64 dye. Fluorescein-conjugated isolectin B4 (IB4) (10 μg/ml) was added to the chamber for 10 min at the end of each FM4-64 experiment, washed out for 10 min and imaged. Only small diameter neurons (<25 μm) were used in analysis of FM4-64 fluorescence changes.

TRG neurons were examined by a Fluoview FV500 confocal laser scanning (CLS) microscopy system (Olympus, Tokyo, Japan) equipped for differential interference contrast microscopy during FM4-64 experiments. The CLS microscopy system was coupled to an upright microscope (IX-71; Olympus) with laser excitation at 568 nm, long-pass emission filter with a cutoff of 590 nm, a ×60 (NA=1.4) oil-immersion objective lens. The scanning rate was 2.0 s/scan for an eight-bit image, 512×512 pixels, in size. Setting for photomultiplier tube, gain, and offset was fixed in all of the experiments. Fluorescence intensities of neurons were analyzed using image analysis software in Fluoview FV500.

Statistical analysis

Results are presented as group means±SEM. Differences in group means were evaluated by RM ANOVA on ranks or *t*-test using the SigmaStat 3.11 software (SYSTAT, San Jose, CA, USA).

RESULTS

In vitro pre-treatment with BoNT decreases KCl-evoked FM4-64 release from somata of acutely isolated TRG neurons

Initially we measured FM4-64 fluorescence intensity by confocal microscopy (2.0 s intervals) before and after KCl stimulation in acutely isolated neurons from naive rats with or without BoNT pre-treatment (BoNT/A was pre-applied *in vitro* for 3 h). We previously reported that the basal decay rate in FM4-64 intensity is dependent on the rate of signal acquisition (photobleaching) and on background vesicular release, which varies between IB4 (+) and IB4 (−) neurons (Matsuka et al., 2007). Since it is impossible to separate bleaching from the background release, the data were not corrected for the basal decay in fluorescence. Application of a depolarizing stimulus (KCl, 75 mM), which allows for robust Ca^{2+} influx via voltage-gated Ca^{2+} channels, increased the rate of FM4-64 signal intensity decrease, reflecting Ca^{2+}-dependent vesicular release of FM4-64 into the extracellular solution (Matsuka et al., 2007). The maximal KCl-induced decreases in FM4-64 signal intensity were also significantly reduced in both types of TRG neurons (Fig. 1). This effect of BoNT/A was significantly greater ($P<0.05$, RM ANOVA on ranks) in IB4 (−) neurons (Fig. 1B) compared to IB4 (+) neurons (Fig. 1A).

Post-treatment with BoNT alleviates IoNC-induced neuropathy behaviors

Next we examined the effect of unilateral IoN constriction on the head withdrawal thresholds (HWTs) of rats to mechanical stimulation in the whisker pad area of IoN innervation. At 14 days after IoNC induction, a large decrease in HWT was observed ipsilateral to IoNC (Fig. 2) without significant changes on the contralateral (sham surgery) side, indicative of tactile allodynia previously demonstrated in this model (Vos et al., 1994). Post-treatment with intradermal ipsilateral injection of BoNT/A (100 pg in 0.1 ml of saline) 3 days after IoNC significantly increased the HWTs (measured at 14 days) compared to saline-injected IoNC rats (Fig. 2).

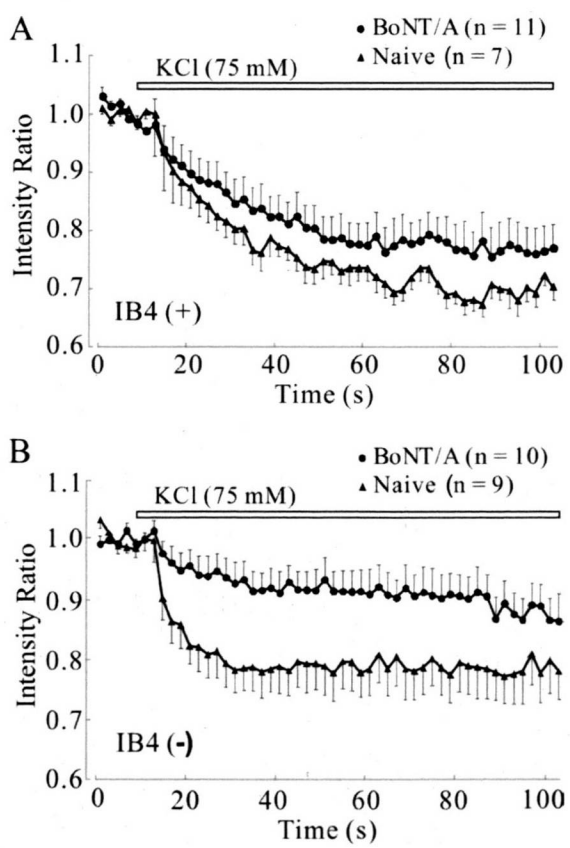

Fig. 1. BoNT/A pre-treatment of dissociated TRG neurons from naive rats decreases KCl-evoked FM4-64 dye release. FM4-64 intensity was measured by confocal microscopy. Pretreatment of TRG neurons with BoNT/A (10 ng/60 μl) for 3 h significantly reduced the rate of KCl-evoked decreases in FM4-64 intensity in both the IB4 (+) (A) and the IB4 (−) (B) neurons compared to untreated neurons.

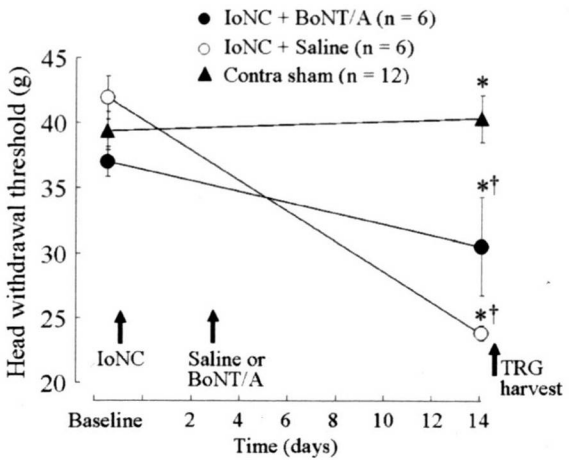

Fig. 2. BoNT/A alleviates the IoNC-induced decreases in withdrawal thresholds to mechanical stimuli. Data are presented as mean±SEM of HWTs to mechanical stimuli measured before (baseline) and 14 days after IoNC. Ipsilateral to, saline-treated IoNC, large >20 g decreases in HWTs were measured at 14 days after IoNC induction. No significant changes in HWTs were observed on the contralateral side. Intradermal BoNT/A injection (100 pg in 0.1 ml of saline) 3 days after IoNC resulted in much smaller (<10 g) decreases in HWTs. * $P<0.05$ between groups; † $P<0.05$ from baseline (RM ANOVA on ranks). Note the large decreases in the slope of the BoNT/A group ($n=6$ rats) compared to the saline group ($n=6$ rats). After behavioral testing, rats were anesthetized and TRG was harvested for FM4-64 release studies.

IoNC speeds up the onset and rate of FM4-64 dye release from somata of TRG neurons

We next studied possible differences in the KCl-induced FM4-64 release in acutely dissociated neurons isolated from TRG ipsilateral to IoNC compared to neurons dissociated from the sham surgery contralateral side. All TRG neurons were isolated at 14 days after IoNC induction in rats studied above (see Fig. 2). IB4 (+) and IB4 (−) neurons ipsilateral to IoNC exhibited a profoundly faster onset of KCl-evoked vesicular release of FM4-64 compared to neurons isolated from contralateral TRG (Fig. 3A, B). The decay time constant (τ) of FM4-64 signal during KCl application was 26.4±8.1 s for IB4 (+) and 11.1±2.6 s for IB4 (−) TRG neurons acutely dissociated from contralateral sham surgery (Fig. 2). IoNC significantly decreased the decay τ in IB4 (+) (3.1±1.0 s) and IB4 (−) (4.2±0.9 s) neurons, without affecting the onset time of KCl-induced vesicular release. In addition, the initial rate of KCl-induced FM4-64 release was faster in IB4 (+) neurons ipsilateral to IoNC (Fig. 3A), while IB4 (−) neurons ipsilateral to IoNC (Fig. 3B) showed significantly larger maximal release of FM4-64 compared to neurons from control rats.

Post-treatment with BoNT decreases the rate and magnitude of FM4-64 dye release from somata of TRG neurons after IoNC

We next studied the effect of post-treatment with BoNT/A on KCl-induced vesicular release of FM4-64 from TRG neurons isolated from rats at 14 days after IoNC. FM4-64 intensity was measured in neurons acutely isolated from TRG ipsilateral to IoNC. We compared FM4-64 release in neurons from IoNC rats treated with BoNT/A with neurons from IoNC rats treated with saline. BoNT or saline was injected into ipsilateral facial skin (100 pg in 0.1 ml of saline) 3 days after the IoNC model induction and 11 days before the dissociation. The KCl-induced decrease in the FM4-64 signal was greatly attenuated in both IB4 (+) and IB4 (−) neurons from IoNC rats treated with peripheral BoNT injection (Fig. 4). Also, the onset of KCl-induced FM4-64 release was significantly slower in both IB4 (+) and IB4 (−) TRG neurons from the BoNT-treated IoNC side.

DISCUSSION

In this study we demonstrated that unilateral IoNC results in long-lasting (>2 weeks) tactile allodynia in the region innervated by the IoN. This is consistent with previous demonstrations that chronic constriction injury of the IoN produces behavioral alterations indicative of trigeminal neuropathic pain (Vos et al., 1994; Idanpaan-Heikkila and Guilbaud, 1999; Kitagawa et al., 2006; Shinoda et al.,

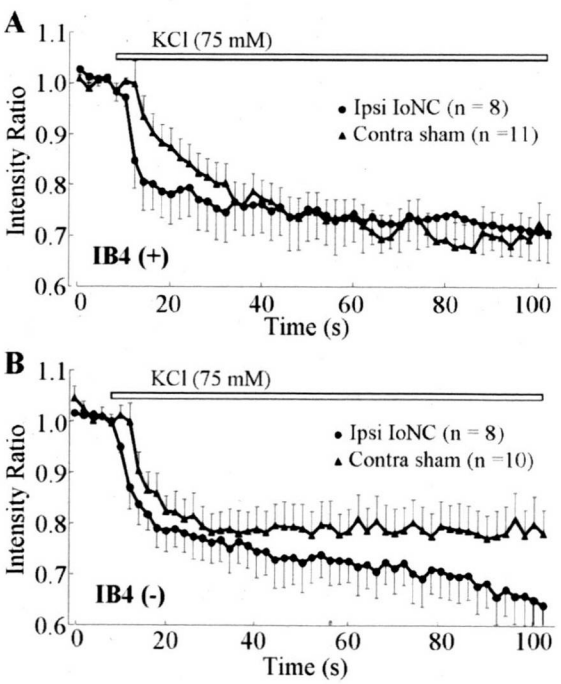

Fig. 3. FM4-64 release in sham (contralateral) and IoNC (ipsilateral) rat TRG neurons. KCl-induced decreases in FM4-64 intensity in acutely dissociated IB4 (+) (A) and IB4 (−) (B) neurons from sham and IoNC sides were measured by confocal microscopy. The onset of KCl-induced vesicular release of FM4-64 is faster in both IB4 (+) and IB4 (−) neurons from the IoNC side compared to the sham contralateral side. In addition, IB4 (−) neurons from the IoNC side exhibited significantly larger maximal decreases in FM4-64 signal compared to contralateral neurons. The decay time constant (τ) of FM4-64 signal during KCl application was 26.4±8.1 s for IB4 (+) and 11.1±2.6 s for IB4 (−) TRG neurons acutely dissociated from contralateral side. IoNC significantly decreased the decay τ in IB4 (+) (3.1±1.0 s) and IB4 (−) (4.2±0.9 s) neurons, without affecting the onset time of KCl-induced vesicular release.

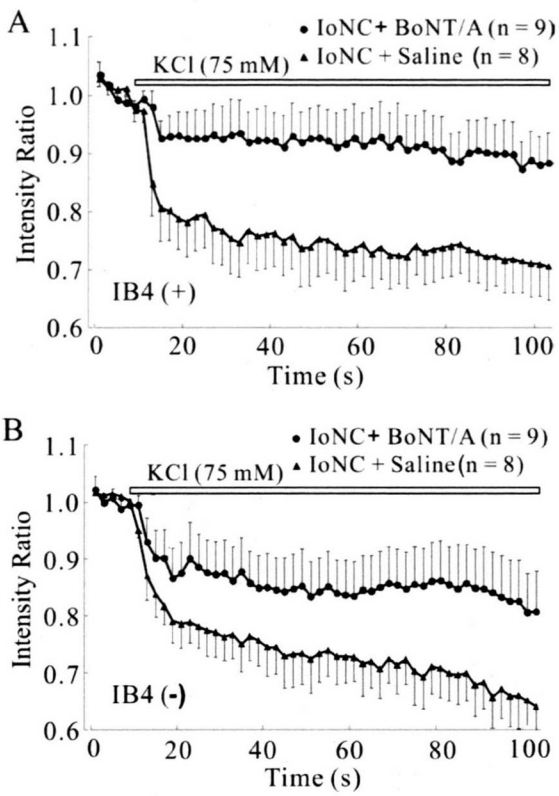

Fig. 4. BoNT/A injection ipsilateral to IoNC decreases vesicular release of FM4-64 from acutely isolated TRG neurons of IoNC rats. BoNT/A (100 pg in 0.1 ml of saline) was injected intradermally in the area of the ipsilateral whisker pad 3 days after IoNC surgery (11 days prior to TRG neuron dissociation). BoNT/A significantly slowed the onset of KCl-induced vesicular FM4-64 release and produced large decreases in maximal release in both IB4 (+) (A) and IB4 (−) (B) neurons compared to neurons from the saline-injected neurons ipsilateral to IoNC.

2007). It is widely acknowledged that persistent hyperexcitability of primary sensory neurons is a major contributor to the development and maintenance of neuropathy behaviors in rodent models of peripheral nerve constriction (reviewed in Gold, 2000; Devor, 2006; Dray, 2008). The demonstrated increases in neurotransmitter release from hyperexcitable afferents within the dorsal horn (Skilling et al., 1992; Mark et al., 1998; Gardell et al., 2003; Coderre et al., 2005) and at the peripheral injury sites (Ma and Quirion, 2006) are also thought to contribute to neuropathic pain, particularly to peripheral and central sensitization. Here we demonstrated that the somata of TRG neurons ipsilateral to IoNC exhibit exaggerated vesicular release of FM4-64. Exaggerated neurotransmitter release from the somata of neurons within sensory ganglia might contribute to increases in chemically-mediated cross-excitation of neighboring neurons after peripheral nerve injury (Devor and Wall, 1990; Amir and Devor, 1996). Peripheral and central terminations of trigeminal afferents would also be expected to exhibit exaggerated neurotransmitter release after IoNC.

With some exceptions, the majority of small diameter (<25 μm) sensory neurons sampled in the present study are considered to be nociceptors (Harper and Lawson, 1985). Mammalian nociceptors have been classified into subclasses based on differential neurotrophin sensitivity and IB4 binding (Bennett et al., 1998). Although some overlap exists, most of the nerve growth factor–responsive IB4 (−) nociceptors contain neuropeptides such as substance P and CGRP, whereas the glial-derived neurotrophic factor–responsive IB4 (+) neurons predominantly lack such neuropeptides (Nagy and Hunt, 1982; Wang et al., 1994; Molliver et al., 1995; Ambalavanar et al., 2003; Fang et al., 2006). Their anatomical distributions also differ in that IB4 (+) neurons innervate the epidermis whereas IB4 (−) neurons innervate subcutaneous and visceral structures (Lu et al., 2001). In the spinal cord, IB4 (+) neurons terminate primarily in the inner lamina II, whereas the IB4 (−) peptidergic nociceptors terminate in lamina I, and outer lamina II (Silverman and Kruger, 1990; Gerke and Plenderleith, 2004; Carlton and Hayes, 1989; Coimbra et al., 1974). Evidence indicates that the IB4 (+) and (−) nociceptor populations are functionally distinct due to the predominant localization of P2X3 receptors on IB4 (+) neurons (Bradbury et al., 1998; Vulchanova et al., 1997, 1998), as well as differences in the magnitudes of TTX-resistant Na^+-currents, Ca^{2+} currents and responses to heat, proton or capsaicin stimuli (Stucky and Lewin, 1999; Dirajlal et al., 2003; Wu and Pan, 2004). However, specific differences exist in IB4 binding and P2X receptor expression between the spinal and trigeminal nociceptive systems (Ambalavanar et al., 2005; Staikopoulos et al., 2007). Previously we demonstrated differences in the patterns of transmitter release and uptake between IB4 (+) and IB4 (−) neurons (Matsuka et al., 2007). In the present study, the initial rate of KCl-induced FM4-64 release was faster in IB4 (+) neurons ipsilateral to IoNC, while IB4 (−) neurons ipsilateral to IoNC showed significantly larger maximal release of FM4-64 compared to neurons from the contralateral (sham surgery) side. Moreover, the onset of KCl-induced vesicular release was faster in both subtypes of TRG neurons ipsilateral to IoNC. Exaggerated neurotransmitter release from sensory neuron terminals after IoNC would be expected to produce larger responses in second order trigeminal brainstem neurons. Such increases in the excitability of pain pathways would then result in the observed tactile allodynia. IoNC-induced alterations in transmitter release from P2X3-containing nociceptors would also be expected to decrease the latency to withdrawal from thermal stimuli observed by others in this neuropathy model (Shinoda et al., 2007).

We did not differentiate between the different innervation targets of the acutely dissociated TRG neurons in our study. However, the profound increase in the onset rate of KCl-evoked vesicular release observed in neurons ipsilateral to IoNC (see Fig. 3) suggests that both injured and uninjured neurons exhibit exaggerated neurotransmitter release after IoNC. In support of this notion, studies have shown that injury of primary afferent neurons results in hyperexcitability of uninjured neurons sharing the same

ganglion (Tsuboi et al., 2004) or peripheral nerve (Ma et al., 2003). However, the precise mechanisms by which increases in excitability and transmitter release might occur in both injured and uninjured neurons remain to be elucidated.

One such mechanism appears to involve alterations in the subunit composition of the N-type voltage-gated calcium channels (N-VGCCs). Spinal nerve ligation results in a marked increase of the $\alpha_2\delta$ subunit expression in sensory neurons that precedes the onset of tactile allodynia (Luo et al., 2001). The anticonvulsant drug, gabapentin, which selectively binds to the $\alpha_2\delta$ subunit of N-VGCCs, decreases tactile allodynia and decreases the enhanced formalin-evoked spinal release of glutamate in this neuropathy model (Coderre et al., 2005). Other selective N-VGCC antagonists also suppress tactile allodynia in this neuropathy model (Chaplan et al., 1994; Calcutt and Chaplan, 1997). Thus, increased neurotransmitter release from sensory neurons might be one of the common underlying mechanisms for chronic pain behaviors following nerve injury.

Cannabinoid analgesics which attenuate neurotransmitter release are also effective in attenuating pain behaviors of many neuropathies (Pertwee, 2001; Di Marzo and Petrocellis, 2006). Unfortunately, their centrally-mediated psychotropic side-effects limit their clinical usefulness. Indeed, this is the case for all of the current medications used to treat neuropathic pain symptoms (Kinloch and Cox, 2005; Dray, 2008). By contrast, clinically detectable centrally-mediated adverse effects are minimal with peripherally administered BoNT/A (Jeynes and Gauci, 2008).

We demonstrated that a 3 h pre-treatment of acutely isolated somata of TRG neurons with BoNT/A significantly decreases their vesicular FM4-64 release (Fig. 1). This decrease in vesicular release was relatively small but consistent with the short (3 h) incubation with BoNT/A. BoNT/A was shown to enter neurons by binding to the synaptic vesicle protein 2A (Dong et al., 2006; Mahrhold et al., 2006); this protein is expressed in somata of TRG neurons (Meng et al., 2007). BoNT/A is then internalized by vesicle endocytosis and translocated into the cytosol where it exerts its proteolytic activity via selective targeting of the synaptosomal-associated protein, 25 kDa (SNAP25) one of the SNARE complex proteins (Schiavo et al., 2000; Rossetto et al., 2006). Studies have shown that overnight or 24 h incubation with BoNT/A causes near-complete inhibition (90%) of KCl-evoked substance P (Welch et al., 2000) or CGRP release (Meng et al., 2007) and an equivalent extent of SNAP25 cleavage in cultured sensory neurons. In our study, BoNT/A produced similar attenuation of vesicular release in both IB4 (+) and IB4 (−) neurons. Our current data also suggest that BoNT/A decreases neurotransmitter release to a similar extent in both subclasses of nociceptors.

We demonstrated that *in vivo* post-treatment of neuropathic rats in the area of IoN innervation with BoNT/A produces profound decreases in vesicular FM4-64 release from ipsilateral TRG neurons acutely dissociated 11 days after BoNT/A injection. These data confirm the persistence of BoNT/A action as well as its retrograde transport in the axons away from the site of injection (Antonucci et al., 2008). It also suggests that retrogradely transported BoNT/A should have reached the central terminals of TRG neurons and attenuated transmitter release from these terminals. Since we did not study the spread of BoNT/A in the brainstem, we could not confirm the demonstrated ability of retrogradely transported BoNT/A to undergo transcytosis (Antonucci et al., 2008). However, the profound decrease in vesicular release of TRG neurons following BoNT/A injection in the whisker pad (Fig. 4) suggests that following retrograde transport transcytosis could occur within the TRG, resulting in the spread of BoNT/A to neurons whose receptive fields are outside the area of BoNT/A injection. Future studies using retrograde markers should help to resolve this issue. Transcytosis of BoNT/A at the central terminals of nociceptive primary afferents might also contribute to the decreases in neuropathy behaviors.

Although our study dealt primarily with nociceptors, we expect that peripheral BoNT/A injection would also decrease transmitter release in the large diameter TRG neurons which normally convey innocuous sensation, thereby affecting transmission of innocuous sensory signals. In neuropathic pain states which involve hyperexcitability and/or sprouting of large diameter myelinated Aβ sensory neurons BoNT/A-induced decreases in transmitter release from these neurons would also contribute to decreasing neuropathy behaviors. Thus, based on the likely indiscriminate effects of BoNT/A on transmitter release in neurons encoding different sensory modalities, clinical use of BoNT/A in neuropathic pain states would have to weigh the benefits of decreasing neuropathic pain symptoms against the disruption of innocuous sensory perception.

CONCLUSIONS

Our data show that unilateral IoNC in rats produces long-lasting behaviors of neuropathy which are concomitant with increased transmitter release from somata of TRG neurons acutely isolated from the side of the injury. We also demonstrate that peripheral injection of BoNT/A alleviates the pain behaviors of IoNC and decreases the exaggerated neurotransmitter release from acutely isolated ipsilateral TRG neurons. The data add to our understanding of neuropathic pain mechanisms and suggest that BoNT/A may represent a valuable alternative to the use of centrally-acting therapeutics for patients with certain types of neuropathic pain.

Acknowledgments—This study was supported by a grant from the Ministry of Education, Science and Culture of Japan (No. 18390512), Ryobi Teien Memorial Foundation and Japanese Association for Dental Science.

REFERENCES

Ambalavanar R, Moritani M, Haines A, Hilton T, Dessem D (2003) Chemical phenotypes of muscle and cutaneous afferent neurons in the rat trigeminal ganglion. J Comp Neurol 460:167–179.

Ambalavanar R, Moritani M, Dessem D (2005) Trigeminal $P2X_3$ receptor expression differs from dorsal root ganglion and is modulated by deep tissue inflammation. Pain 117:280–291.

Amir R, Devor M (1996) Chemically mediated cross-excitation in rat dorsal root ganglia. J Neurosci 16:4733–4741.

Antonucci F, Rossi C, Gianfranceschi L, Rossetto O, Caleo M (2008) Long-distance retrograde effects of botulinum neurotoxin A. J Neurosci 28:3689–3696.

Bach-Rojecky L, Relja M, Lackovic Z (2005) Botulinum toxin type A in experimental neuropathic pain. J Neural Transm 112:215–219.

Bennett GJ, Xie YK (1988) A peripheral mononeuropathy in rat that produces disorders of pain sensation like those seen in man. Pain 33:87–107.

Bennett DL, Michael GJ, Ramachandran N, Munson JB, Averill S, Yan Q, McMahon SB, Priestley JV (1998) A distinct subgroup of small DRG cells express GDNF receptor components and GDNF is protective for these neurons after nerve injury. J Neurosci 18:3059–3072.

Bradbury EJ, Burnstock G, McMahon SB (1998) The expression of P2X3 purinoreceptors in sensory neurons: effects of axotomy and glial-derived neurotrophic factor. Mol Cell Neurosci 12:256–268.

Calcutt NA, Chaplan SR (1997) Spinal pharmacology of tactile allodynia in diabetic rats. Br J Pharmacol 122:1478–1482.

Carlton SM, Hayes ES (1989) Dynorphin A(1-8) immunoreactive cell bodies, dendrites and terminals are postsynaptic to calcitonin gene-related peptide primary afferent terminals in the monkey dorsal horn. Brain Res 504:124–128.

Chaplan SR, Pogrel JW, Yaksh TL (1994) Role of voltage-dependent calcium channel subtypes in experimental tactile allodynia. J Pharmacol Exp Ther 269:1117–1123.

Coderre TJ, Kumar N, Lefebvre CD, Yu JS (2005) Evidence that gabapentin reduces neuropathic pain by inhibiting the spinal release of glutamate. J Neurochem 94:1131–1139.

Coimbra A, Sodré-Borges BP, Magalhães MM (1974) The substantia gelatinosa Rolandi of the rat. Fine structure, cytochemistry (acid phosphatase) and changes after dorsal root section. J Neurocytol 3:199–217.

Cui M, Khanijou S, Rubino J, Aoki KR (2004) Subcutaneous administration of botulinum toxin A reduces formalin-induced pain. Pain 107:125–133.

Devor M (2006) Sodium channels and mechanisms of neuropathic pain. J Pain 7:S3–S12.

Devor M, Wall PD (1990) Cross-excitation in dorsal root ganglia of nerve-injured and intact rats. J Neurophysiol 64:1733–1746.

Di Marzo V, Petrocellis LD (2006) Plant, synthetic, and endogenous cannabinoids in medicine. Annu Rev Med 57:553–574.

Dirajlal S, Pauers LE, Stucky CL (2003) Differential response properties of IB(4)-positive and -negative unmyelinated sensory neurons to protons and capsaicin. J Neurophysiol 89:513–524.

Dong M, Yeh F, Tepp WH, Dean C, Johnson EA, Janz R, Chapman ER (2006) SV2 is the protein receptor for botulinum neurotoxin A. Science 312:592–596.

Dray A (2008) Neuropathic pain: emerging treatments. Br J Anaesth 101:48–58.

Durham PL, Cady R, Cady R (2004) Regulation of calcitonin gene-related peptide secretion from trigeminal nerve cells by botulinum toxin type a: implications for migraine therapy. Headache 44:35–42.

Fang X, Djouhri L, McMullan S, Berry C, Waxman SG, Okuse K, Lawson SN (2006) Intense isolectin-B4 binding in rat dorsal root ganglion neurons distinguishes C-fiber nociceptors with broad action potentials and high Nav1.9 expression. J Neurosci 26:7281–7292.

Fromm GH (1989) Trigeminal neuralgia and related disorders. Neurol Clin 7:305–319.

Gardell LR, Vanderah TW, Gardell SE, Wang R, Ossipov MH, Lai J, Porreca F (2003) Enhanced evoked excitatory transmitter release in experimental neuropathy requires descending facilitation. J Neurosci 23:8370–8379.

Gerke MB, Plenderleith MB (2004) Analysis of the unmyelinated primary sensory neurone projection through the dorsal columns of the rat spinal cord using transganglionic transport of the plant lectin Bandeiraea simplicifolia I-isolectin B4. J Neurol Sci 221:69–77.

Gold MS (2000) Spinal nerve ligation: what to blame for the pain and why. Pain 84:117–120.

Harper AA, Lawson SN (1985) Electrical properties of rat dorsal root ganglion neurons with different peripheral nerve conduction velocities. J Physiol (Lond) 359:47–63.

Huang LY, Neher E (1996) Ca(2+)-dependent exocytosis in the somata of dorsal root ganglion neurons. Neuron 17:135–145.

Idanpaan-Heikkila JJ, Guilbaud G (1999) Pharmacological studies on a rat model of trigeminal neuropathic pain: baclofen, but not carbamazepine, morphine or tricyclic antidepressants, attenuates the allodynia-like behaviour. Pain 79:281–290.

Ishikawa H, Mitsui Y, Yoshitomi T, Mashimo K, Aoki S, Mukuno K, Shimizu K (2000) Presynaptic effects of botulinum toxin type a on the neuronally evoked response of albino and pigmented rabbit iris sphincter and dilator muscles. Jpn J Ophthalmol 44:106–109.

Jeynes LC, Gauci CA (2008) Evidence for the use of botulinum toxin in the chronic pain setting—a review of the literature. Pain Pract 8:269–276.

Kajander KC, Wakisaka S, Bennett GJ (1992) Spontaneous discharge originates in the dorsal root ganglion at the onset of a painful peripheral neuropathy in the rat. Neurosci Lett 138:225–228.

Kim SH, Chung JM (1992) An experimental model for peripheral neuropathy produced by segmental spinal nerve ligation in the rat. Pain 50:355–363.

Kinloch RA, Cox PJ (2005) New targets for neuropathic pain therapeutics. Expert Opin Ther Targets 9:685–698.

Kirk EJ (1974) Impulses in dorsal spinal nerve rootlets in cats and rabbits arising from dorsal root ganglia isolated from the periphery. J Comp Neurol 155:165–175.

Kitagawa J, Takeda M, Suzuki I, Kadoi J, Tsuboi Y, Honda K, Matsumoto S, Nakagawa H, Tanabe A, Iwata K (2006) Mechanisms involved in modulation of trigeminal primary afferent activity in rats with peripheral mononeuropathy. Eur J Neurosci 24:1976–1986.

Lee JC, Yokoyama T, Hwang HJ, Arimitsu H, Yamamoto Y, Kawasaki M, Takigawa T, Takeshi K, Nishikawa A, Kumon H, Oguma K (2007) Clinical application of Clostridium botulinum type A neurotoxin purified by a simple procedure for patients with urinary incontinence caused by refractory destrusor overactivity. FEMS Immunol Med Microbiol 51:201–211.

Li JX, Zhao WL, Liang JH (2004) Effects of carbamazepine on morphine-induced behavioral sensitization in mice. Brain Res 1019:77–83.

Lu J, Zhou XF, Rush RA (2001) Small primary sensory neurons innervating epidermis and viscera display differential phenotype in the adult rat. Neurosci Res 41:355–363.

Luo ZD, Chaplan SR, Higuera ES, Sorkin LS, Stauderman KA, Williams ME, Yaksh TL (2001) Upregulation of dorsal root ganglion (alpha)2(delta) calcium channel subunit and its correlation with allodynia in spinal nerve-injured rats. J Neurosci 21:1868–1875.

Luvisetto S, Marinelli S, Cobianchi S, Pavone F (2007) Antiallodynic efficacy of botulinum neurotoxin A in a model of neuropathic pain. Neuroscience 145:1–4.

Luvisetto S, Marinelli S, Lucchetti F, Marchi F, Cobianchi S, Rossetto O, Montecucco C, Pavone F (2006) Botulinum neurotoxins and formalin-induced pain: central vs. peripheral effects in mice. Brain Res 1082:124–131.

Ma C, Shu Y, Zheng Z, Chen Y, Yao H, Greenquist KW, White FA, LaMotte RH (2003) Similar electrophysiological changes in axotomized and neighboring intact dorsal root ganglion neurons. J Neurophysiol 89:1588–1602.

Ma W, Quirion R (2006) Increased calcitonin gene-related peptide in neuroma and invading macrophages is involved in the upregulation of interleukin-6 and thermal hyperalgesia in a rat model of mononeuropathy. J Neurochem 98:180–192.

Mahrhold S, Rummel A, Bigalke H, Davletov B, Binz T (2006) The synaptic vesicle protein 2C mediates the uptake of botulinum neurotoxin A into phrenic nerves. FEBS Lett 580:2011–2014.

Mark MA, Colvin LA, Duggan AW (1998) Spontaneous release of immunoreactive neuropeptide Y from the central terminals of large diameter primary afferents of rats with peripheral nerve injury. Neuroscience 83:581–589.

Matsuka Y, Neubert JK, Maidment NT, Spigelman I (2001) Concurrent release of ATP and substance P within guinea pig trigeminal ganglia in vivo. Brain Res 915:248–255.

Matsuka Y, Edmonds B, Mitrirattanakul S, Schweizer FE, Spigelman I (2007) Two types of neurotransmitter release patterns in isolectin B4-positive and negative trigeminal ganglion neurons. Neuroscience 144:665–674.

Meng J, Wang J, Lawrence G, Dolly JO (2007) Synaptobrevin I mediates exocytosis of CGRP from sensory neurons and inhibition by botulinum toxins reflects their antinociceptive potential. J Cell Sci 120:2864–2874.

Molliver DC, Radeke MJ, Feinstein SC, Snider WD (1995) Presence or absence of TrkA protein distinguishes subsets of small sensory neurons with unique cytochemical characteristics and dorsal horn projections. J Comp Neurol 361:404–416.

Mosconi T, Kruger L (1996) Fixed-diameter polyethylene cuffs applied to the rat sciatic nerve induce a painful neuropathy: ultrastructural morphometric analysis of axonal alterations. Pain 64:37–57.

Nagy JI, Hunt SP (1982) Fluoride-resistant acid phosphatase-containing neurones in dorsal root ganglia are separate from those containing substance P or somatostatin. Neuroscience 7:89–97.

Neubert JK, Maidment NT, Matsuka Y, Adelson DW, Kruger L, Spigelman I (2000) Inflammation-induced changes in primary afferent-evoked release of substance P within trigeminal ganglia in vivo. Brain Res 871:181–191.

Niemann H, Blasi J, Jahn R (1994) Clostridial neurotoxins: new tools for dissecting exocytosis. Trends Cell Biol 4:179–185.

Oh EJ, Weinreich D (2002) Chemical communication between vagal afferent somata in nodose ganglia of the rat and the guinea pig in vitro. J Neurophysiol 87:2801–2807.

Pertwee RG (2001) Cannabinoid receptors and pain. Prog Neurobiol 63:569–611.

Rappaport ZH, Devor M (1994) Trigeminal neuralgia: the role of self-sustaining discharge in the trigeminal ganglion. Pain 56:127–138.

Rossetto O, Morbiato L, Caccin P, Rigoni M, Montecucco C (2006) Presynaptic enzymatic neurotoxins. J Neurochem 97:1534–1545.

Schiavo G, Matteoli M, Montecucco C (2000) Neurotoxins affecting neuroexocytosis. Physiol Rev 80:717–766.

Seltzer Z, Dubner R, Shir Y (1990) A novel behavioral model of neuropathic pain disorders produced in rats by partial sciatic nerve injury. Pain 43:205–218.

Sheen K, Chung JM (1993) Signs of neuropathic pain depend on signals from injured nerve fibers in a rat model. Brain Res 610:62–68.

Shinoda M, Kawashima K, Ozaki N, Asai H, Nagamine K, Sugiura Y (2007) P2X3 receptor mediates heat hyperalgesia in a rat model of trigeminal neuropathic pain. J Pain 8:588–597.

Silverman JD, Kruger L (1990) Analysis of taste bud innervation based on glycoconjugate and peptide neuronal markers. J Comp Neurol 292:575–584.

Skilling SR, Harkness DH, Larson AA (1992) Experimental peripheral neuropathy decreases the dose of substance P required to increase excitatory amino acid release in the CSF of the rat spinal cord. Neurosci Lett 139:92–96.

Staikopoulos V, Sessle BJ, Furness JB, Jennings EA (2007) Localization of P2X2 and P2X3 receptors in rat trigeminal ganglion neurons. Neuroscience 144:208–216.

Stucky CL, Lewin GR (1999) Isolectin B(4)-positive and -negative nociceptors are functionally distinct. J Neurosci 19:6497–6505.

Tsuboi Y, Takeda M, Tanimoto T, Ikeda M, Matsumoto S, Kitagawa J, Teramoto K, Simizu K, Yamazaki Y, Shima A, Ren K, Iwata K (2004) Alteration of the second branch of the trigeminal nerve activity following inferior alveolar nerve transection in rats. Pain 111:323–334.

Ulrich-Lai YM, Flores CM, Harding-Rose CA, Goodis HE, Hargreaves KM (2001) Capsaicin-evoked release of immunoreactive calcitonin gene-related peptide from rat trigeminal ganglion: evidence for intraganglionic neurotransmission. Pain 91:219–226.

Vos BP, Strassman AM, Maciewicz RJ (1994) Behavioral evidence of trigeminal neuropathic pain following chronic constriction injury to the rat's infraorbital nerve. J Neurosci 14:2708–2723.

Vulchanova L, Riedl MS, Shuster SJ, Stone LS, Hargreaves KM, Buell G, Surprenant A, North RA, Elde R (1998) P2X3 is expressed by DRG neurons that terminate in inner lamina II. Eur J Neurosci 10:3470–3478.

Vulchanova L, Riedl MS, Shuster SJ, Buell G, Surprenant A, North RA, Elde R (1997) Immunohistochemical study of the P2X2 and P2X3 receptor subunits in rat and monkey sensory neurons and their central terminals. Neuropharmacology 36:1229–1242.

Wang H, Rivero-Melian C, Robertson B, Grant G (1994) Transganglionic transport and binding of the isolectin B4 from *Griffonia simplicifolia* I in rat primary sensory neurons. Neuroscience 62: 539–551.

Welch MJ, Purkiss JR, Foster KA (2000) Sensitivity of embryonic rat dorsal root ganglia neurons to *Clostridium botulinum* neurotoxins. Toxicon 38:245–258.

Wu ZZ, Pan HL (2004) Tetrodotoxin-sensitive and -resistant Na^+ channel currents in subsets of small sensory neurons of rats. Brain Res 1029:251–258.

Xie Y, Zhang J, Petersen M, LaMotte RH (1995) Functional changes in dorsal root ganglion cells after chronic nerve constriction in the rat. J Neurophysiol 73:1811–1820.

Zakrzewska JM, Patsalos PN (1992) Drugs used in the management of trigeminal neuralgia. Oral Surg Oral Med Oral Pathol 74:439–450.

Zhang JM, Song XJ, LaMotte RH (1997) An in vitro study of ectopic discharge generation and adrenergic sensitivity in the intact, nerve-injured rat dorsal root ganglion. Pain 72:51–57.

(Accepted 29 January 2009)
(Available online 3 February 2009)

Simvastatin Induces the Odontogenic Differentiation of Human Dental Pulp Stem Cells *In Vitro* and *In Vivo*

Yosuke Okamoto, DDS, Wataru Sonoyama, DDS, PhD,* Mitsuaki Ono, DDS, PhD,* Kentaro Akiyama, DDS, PhD,*† Takuo Fujisawa, DDS, PhD,* Masamitsu Oshima, DDS,* Yohei Tsuchimoto, DDS, PhD,* Yoshizo Matsuka, DDS, PhD,* Tatsuji Yasuda, MD, PhD,‡ Songtao Shi, DDS, PhD,† and Takuo Kuboki, DDS, PhD**

Abstract

Statin, 3-hydroxy-3-methylglutaryl coenzyme A reductase inhibitor, is known to promote bone formation. However, it is not clear whether statin affects the differentiation of pulp cells. This study used a cell proliferation assay, cell cycle analysis, quantitative reverse transcriptase polymerase chain reaction (RT-PCR) and *in vivo* transplantation to examine the effects of simvastatin on human dental pulp stem cells (DPSCs) *in vitro* and *in vivo*. Simvastatin at 1 μmol/L was able to significantly suppress the proliferation of DPSCs without inducing apoptosis. Quantitative RT-PCR revealed both osteocalcin and dentin sialophosphoprotein to be significantly up-regulated when DPSCs were cultured with simvastatin in comparison to bone morphogenetic protein-2 treatment. The *in vivo* transplantation data showed that simvastatin treatment promoted mineralized tissue formation. Taken together, these results suggest that statin might be an ideal active ingredient to accelerate the differentiation of DPSCs. *(J Endod 2009;35:367–372)*

Key Words

Cell differentiation, cell proliferation, dental pulp stem cells, dentin regeneration, pulp capping material, reparative dentin formation, simvastatin

From the *Department of Oral Rehabilitation and Regenerative Medicine and ‡Department of Cell Chemistry, Okayama University Graduate School of Medicine, Dentistry, and Pharmaceutical Sciences, Okayama, Japan; and †Center for Craniofacial Molecular Biology, University of Southern California School of Dentistry, Los Angeles, California.

Address requests for reprints to Takuo Kuboki, DDS, PhD, Department of Oral Rehabilitation and Regenerative Medicine, Okayama University Graduate School of Medicine, Dentistry and Pharmaceutical Sciences, 2-5-1 Shikata-cho, Okayama 700-8525, Japan. E-mail address: kuboki@md.okayama-u.ac.jp.
0099-2399/$0 - see front matter

doi:10.1016/j.joen.2008.11.024

Nonsurgical endodontic treatment, eg, a pulpectomy, is initially selected for the treatment of irreversible pulpitis. It is reported that 97% of teeth were retained in the oral cavity 8 years after the initial nonsurgical endodontic treatment (1). However, the frequency of clinical complications, including apical periodontitis and root fracture, has been reported to increase in endodontically treated teeth in comparison to vital teeth (2, 3). Therefore, treatment to maintain pulp vitality and function (vital pulp therapy) is used to avoid totally irreversible pulpitis that would certainly result in a pulpectomy. Although calcium hydroxide is conventionally used as a pulp capping material for vital pulp therapy, its long-term success rate varies among reports and is sometimes unsatisfactory (4, 5). One of the reasons for these unpredictable results is that calcium hydroxide does not biologically activate odontoblasts or accelerate reparative dentin formation (6). Therefore, the development of pulp capping materials with the biologic ability to activate odontoblasts and accelerate dentin formation is important. However, so far, no optimal pulp capping materials with excellent long-term clinical outcome have been developed.

In an experimental setting, several growth factors were investigated and proved to induce odontogenic differentiation of dental pulp cells *in vitro* and to accelerate dentin formation *in vivo* (7–12). Among them, bone morphogenetic proteins (BMPs) were considered to be promising growth factors capable of promoting odontogenic differentiation (9–11). However, the possibility of unexpected side effects and the production cost can be obstacles for their clinical application.

Statin, 3-hydroxy-3-methylglutaryl coenzyme A reductase inhibitor, is the first-line drug for hyperlipidemia, and it has been recognized to be a safe and low-priced drug as a result of its worldwide longtime usage. Statin has multiple functions including anti-inflammation, induction of angiogenesis, and improvement of the vascular endothelial cell function (13–16). Another interesting and important function of statin is its effect on bone formation. Statin improves the osteoblast function via the BMP-2 pathway and suppresses osteoclast function, resulting in enhanced bone formation (17–19). Therefore, statin might improve the function of odontoblasts, thus leading to improved dentin formation. However, the effects of statin on odontoblastic cells have not yet been reported.

The purpose of this study was to examine the effects of statin on the behavior of human dental pulp stem cells (DPSCs) (20–22) in terms of cell proliferation, cell cycle, gene expression patterns, and *in vivo* tissue formation.

Materials and Methods

Sample Collection and Cell Culture

Seven third molars were collected from 5 adults (22–26 years old) at Okayama University Hospital under the approved guidelines and protocol (Okayama University Ethics Committee #418 and 433), with written informed consent obtained from all subjects . The isolation and culture of human DPSCs were performed according to the method previously described (20–22). In brief, pulp tissue was gently and aseptically separated from the extracted teeth, minced, and digested in a solution of 3 mg/mL collagenase type I (Invitrogen, Carlsbad, CA) and 4 mg/mL dispase (Invitrogen) for approximately 1 hour at 37°C. Single-cell suspensions were obtained by passing the

solution through a 70 μm strainer, seeded at 1×10^4 cells/10-cm culture plate, and cultured with complete medium consisting of α-MEM (Sigma Chemical Company, St Louis, MO), 15% fetal bovine serum (FBS; Cancera International Inc, Ontario, Canada), 100 mmol/L L-ascorbic acid 2-phosphate (Sigma Chemical Company), 2 mmol/L L-glutamine (Sigma Chemical Company), 100 units/mL penicillin (Meiji Seika, Tokyo, Japan), and 100 mg/mL streptomycin (Meiji Seika) at 37°C under 5% CO_2 in air. DPSCs at 3–6 passages were confirmed to express dentin sialophosphoprotein (*dspp*) by reverse transcriptase polymerase chain reaction (RT-PCR) and used in this study (23).

Simvastatin (Calbiochem, San Diego, CA) was used as a typical statin in this study, and its stock solution was prepared according to the manufacturer's instructions. BMP-2 was purchased from R&D Systems Inc (Minneapolis, MN) and used as a positive control. Each experiment *in vitro* and *in vivo* was repeated at least twice, and the reproducibility for each was also confirmed.

Evaluation of Cell Proliferation

DPSCs were seeded onto 96-well plastic culture plates at 2.0×10^4 cells/well with complete medium. Twenty-four hours after seeding, the medium was changed to complete medium supplemented with simvastatin (0.1, 1, or 10 μmol/L) or BMP-2 (100 ng/mL). At 1, 3, and 5 days after simvastatin or BMP-2 addition, the MTS assay was carried out to evaluate the number of viable cells (CellTiter 96 Aqueous One Solution; Promega, Madison, WI) according to the manufacturer's instructions (24). The proliferation efficiency was determined from data obtained by measuring the optical absorbance at a wavelength of 490 nm with a microplate reader (Bio Rad, Hercules, CA). The mean values obtained from 8 wells under each condition were computed and statistically analyzed.

Mevalonate (Sigma Chemical Company) was used to confirm whether the effect of statin on DPSCs was mediated via the mevalonate pathway. DPSCs were cultured with complete medium supplemented mevalonate (1 mmol/L) (25) and/or simvastatin (1 μmol/L) for 5 days. Thereafter, an MTS assay was performed to evaluate the number of viable cells.

Evaluation of Fiber Formation

To evaluate the effect on fiber formation, DPSCs at the subconfluent stage were cultured with serum-free medium for 3 days. Next, simvastatin (1 or 10 μmol/L) or BMP-2 (100 ng/mL) was added to the medium, and the cells were cultured for 2 days. The actin fibers were stained with phalloidin-TRITC (Sigma Chemical Company), and the nuclei were stained with DAPI (Invitrogen), and thereafter they were observed under a fluorescence microscope.

Cell Cycle Analysis

The cell cycle and DNA fragmentation was analyzed by fluorescence-activated cell sorter (FACS) (FACSCalibur; Becton Dickinson, Franklin Lakes, NJ). In brief, DPSCs cultured with simvastatin (1 μmol/L) for 3 days were collected and stained with propidium iodide (200 ng/mL) (Calbiochem) and then subjected to a FACS analysis. H_2O_2 (0.3 mmol/L) was used as an apoptosis inducer (26) or a positive control in this experiment.

Quantitative RT-PCR Analysis

Total cellular RNA was extracted from DPSCs cultured with simvastatin (0.1, or 1 μmol/L) for 7 days by RNeasy (QIAGEN, Hilden, Germany) according to the manufacturer's instructions. RNA samples were reverse transcribed by using the Transcriptor First Strand cDNA Synthesis Kit (Roche Molecular Biochemicals, Mannheim, Germany). Quantitative RT-PCR was performed to quantify the gene expression level of odontoblastic markers by using a specified thermal cycler (LightCycler; Roche Molecular Biochemicals) with SYBR Green reagent (Roche Molecular Biochemicals). These genes included glyceraldehyde-3-phosphate dehydrogenase (*gapdh*), *dspp*, and osteocalcin (*ocn*). The samples were subjected to 40 cycles of amplification at 95°C for 15 seconds followed by 64°C for 20 seconds and 72°C for 25 seconds by using the specific primers (Table 1). The results of the assays were normalized to the level of *gapdh*.

TABLE 1. Primer Sequences for Quantitative RT-PCR

Gene name (accession no.)		Primer sequences
gapdh (NM002046)	Forward	5′-CCATGGAGAAGGCTGGG-3′
	Reverse	5′-CAAAGTTGTCATGGATGACC-3′
dspp (NM14208)	Forward	5′-GTGATAGAGGAAGGCAAGAG-3′
	Reverse	5′-ATTCCAGCCCTCAATATTCC-3′
ocn (NM199173)	Forward	5′-CAAAGGTGCAGCCTTTGTGTC-3′
	Reverse	5′-TCACAGTCCGGATTGAGCTCA-3′

In Vivo Transplantation and Histologic Examination

DPSCs were cultured with simvastatin (0.1 or 1 μmo/L) or BMP-2 (100 ng/mL) for 7 days. Next, approximately 4.0 x 10^6 *ex vivo* expanded DPSCs were mixed with 40 mg of hydroxyapatite/tricalcium phosphate (HA/TCP) ceramic powder (Zimmer Inc, Warsaw, IN) and then transplanted subcutaneously into the dorsal surface of 10-week-old immunocompromised mice (NIH-bg-nu/nu-xid; Harlan Sprague Dawley, Indianapolis, IN) as previously described (20, 21, 27). These procedures were performed in accordance with the specifications of an approved animal protocol (Okayama University #OKU-2007226 and University of Southern California #10874). The transplants were recovered at 8 weeks after transplantation, fixed with 4% paraformaldehyde, decalcified with buffered 10% ethylenediaminetetraacetic acid, and then embedded in paraffin. Sections were deparaffinized and stained with hematoxylin-eosin. For the quantification of newly formed mineralized tissue *in vivo*, NIH Image software (http://rsb.info.nih.gov/nih-image) was used. The mineralized tissue area rate was calculated as the percentage of mineralized tissue area per total area at 4 representative areas from each group.

Statistical Analysis

One-way factorial analysis of variance (ANOVA) followed by Fisher PLDS tests were used for the statistical analysis (StatView; SAS Institute, Cary, NC). *P* values of less than .05 were considered to be statistically significant. All statistical data were presented as the mean ± standard deviation.

Results

Simvastatin Suppressed the Proliferation of DPSCs

Fig. 1 represents the effect of simvastatin on the proliferation of DPSCs. Simvastatin at 0.1 μmol/L and BMP-2 had no effects on the proliferation until 5 days in culture. However, simvastatin at 10 μmol/L significantly suppressed the proliferation in day-3 and day-5 cultures in comparison to the control. Simvastatin at 1 μmol/L also significantly suppressed the proliferation in a day-5 culture. These cells were stained by 0.5% trypan blue, and the stained cells were counted to evaluate the ratio of dead cells in each group. The ratio of dead cells in the cells treated by simvastatin at 10 μmol/L groups was 56.4% and

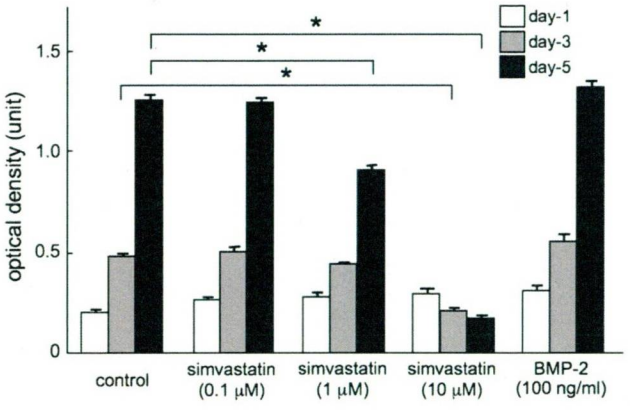

Figure 1. Simvastatin suppressed the proliferation of DPSCs. When simvastatin was added to the culture of DPSCs, the proliferation was significantly suppressed in day-3 (at 10 μmol/L) and day-5 cultures (at 1 and 10 μmol/L). BMP-2 did not affect the proliferation of DPSCs (n = 8, One-way factorial ANOVA followed by Fisher PLDS tests; *$P < .0001$).

much higher than other groups (control, 21.2%; simvastatin at 0.1 μmol/L, 25.3%; simvastatin at 1 μmol/L, 20.2%; BMP-2, 30.5%).

To confirm the putative pathway of this suppression, 3 experiments were conducted. At first, mevalonate was added to the culture in addition to simvastatin (1 μmol/L) and found to restore the proliferation (Fig. 2*A*). Next, actin fiber formation, as a downstream pathway of Rho, was confirmed by phalloidin staining (Fig. 2*B*). In a day-3 culture, simvastatin at 1 μmol/L slightly suppressed the actin fiber formation. Obvious suppression of fiber formation was observed in the culture treated by simvastatin at 10 μmol/L. The effect of BMP-2 on fiber formation was not evident. Third, the cell cycle was analyzed by FACS (Fig. 2*C*). The treatment by simvastatin at 1 μmol/L led to a decrease of the peak of the cells in the G2/M phase. H_2O_2 treatment also led to a decrease of the peak of the cells in the G2/M phase. However, at the same time, H_2O_2 treatment resulted in the accumulation of the cells in the apoptotic sub-G1 phase, which was not observed in the simvastatin-treated cells.

Simvastatin Induced Odontogenic Gene Expression in DPSCs

The gene expression levels of odontogenic markers, *dspp* and *ocn*, were analyzed in a day-7 culture by quantitative RT-PCR (Fig. 3). Simvastatin at 1 μmol/L induced *dspp* gene expression up to 3.7 times significantly in comparison to the control. The induction of *dspp* gene expression by BMP-2 was not significantly different in comparison to the control. The *ocn* gene expression was also up-regulated by simvastatin at 1 μmol/L up to 18.1 times in comparison to the control. BMP-2 also up-regulated *ocn* gene expression significantly

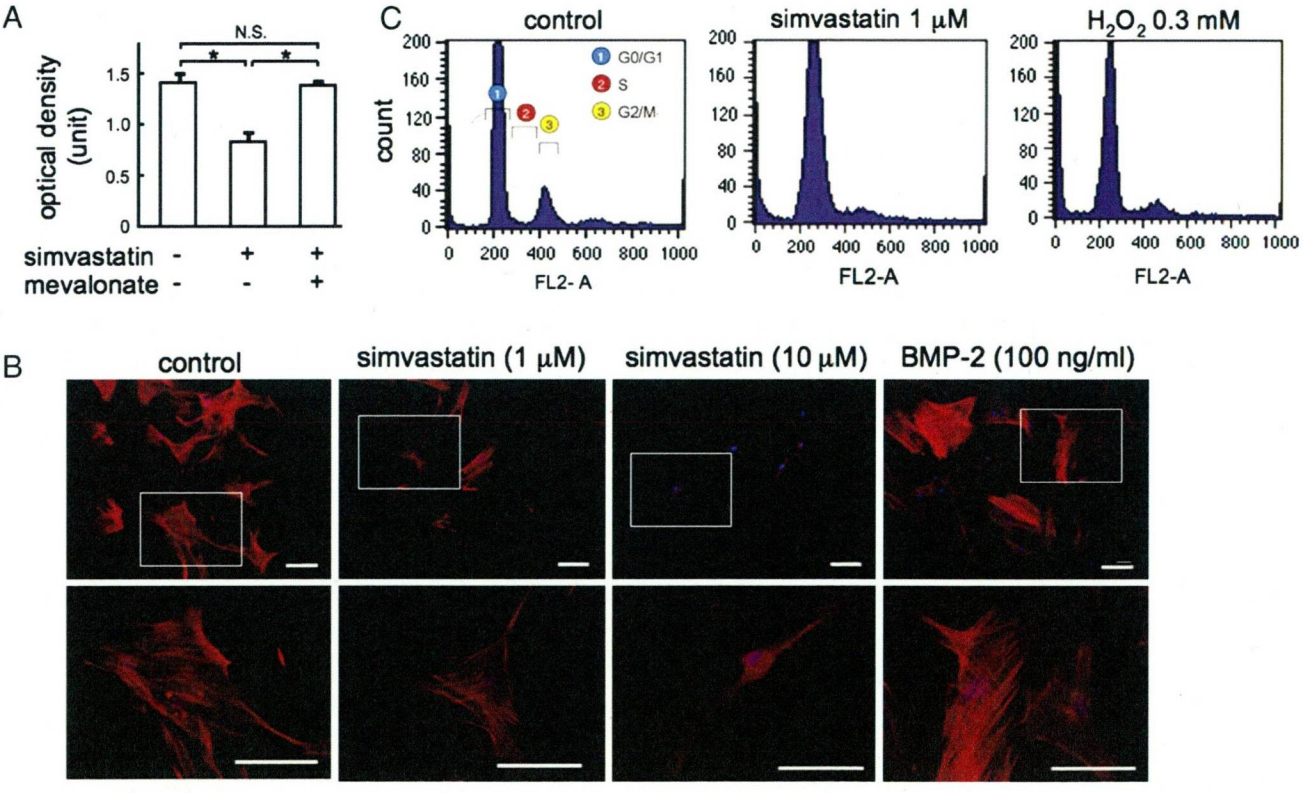

Figure 2. The suppression of the proliferation was a result of G1 arrest but not apoptosis that was mediated via the mevalonate and Rho pathways. (*A*) The proliferation was suppressed when simvastatin was added at 1 μmol/L to the culture for 5 days. However, when mevalonate was added at 1 mmol/L to the culture together with simvastatin, the suppression was restored (n = 8, one-way factorial ANOVA followed by Fisher PLDS tests; *$P < .001$, NS). (*B*) The actin fiber formation was suppressed slightly by simvastatin at 1 μmol/L and significantly by simvastatin at 10 μmol/L. BMP-2 did not affect the actin fiber formation. The white square in each upper panel indicates the region of each corresponding lower panel. Representative images are shown (scale bar, 100 μm). (*C*) The treatment by simvastatin at 1 μmol/L led to a decrease of the peak of the cells in the G2/M phase. H_2O_2 treatment also led to a decrease of the peak for the cells in the G2/M phase. However, at the same time, H_2O_2 treatment resulted in the accumulation of the cells in the apoptotic sub-G1 phase that was not observed in the simvastatin-treated cells.

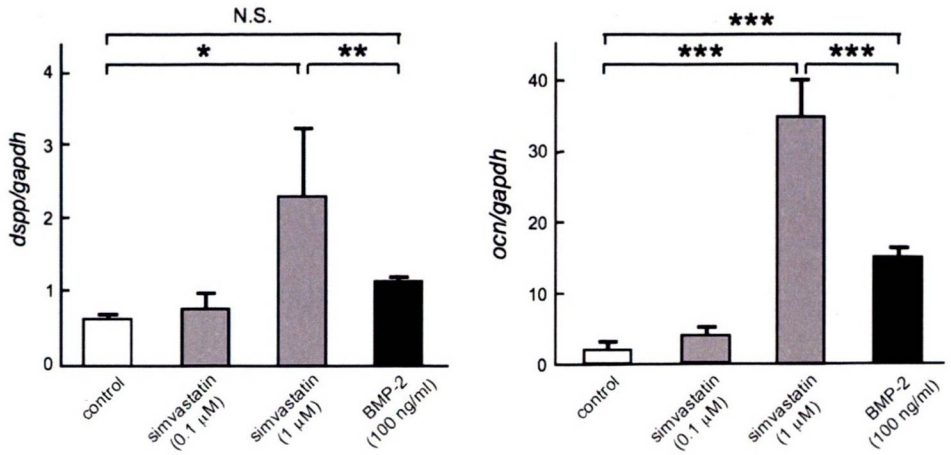

Figure 3. Simvastatin induced odontogenic gene expression in DPSCs. Simvastatin at 1 μmol/L induced *dspp* gene expression in a day-7 culture up to 3.7 times in comparison to the control. The induction of *dspp* gene expression by BMP-2 was not significant in comparison to the control. *ocn* gene expression was also up-regulated by simvastatin at 1 μmol/L in day 7 culture up to 18.1 times in comparison to the control. BMP-2 up-regulated *ocn* gene expression significantly higher than the control. However, the induction by simvastatin was significantly higher than that by BMP-2 (n = 8, one-way factorial ANOVA followed by Fisher PLDS tests: $*P < .01$, $**P < .05$, $***P < .0001$, N.S.=not significant).

higher than the control. However, the induction by simvastatin was significantly higher than that by BMP-2.

Simvastatin Accelerated DPSC-Mediated Mineralized Tissue Formation *In Vivo*

DPSCs were treated by simvastatin or BMP-2 and then transplanted into immunocompromised mice to evaluate the effects on mineralized tissue formation (Fig. 4). Although all groups, including the control, showed mineralized tissue formation after 8 weeks, DPSCs pretreated by simvastatin at 1 μmol/L or BMP-2 for 7 days formed a significantly larger amount of mineralized tissue in comparison to others (Fig. 4*E*).

Discussion

DPSCs possess postnatal stem cell characteristics, including multipotent differentiation, self-renewal, clonogenic capacity, and expression of multiple mesenchymal stem cell surface markers (20, 21, 28). DPSCs are also a heterogenic stem cell analogous to bone marrow mesenchymal stem cells (BMMSCs) (20–22). One of the unique characteristics of DPSCs is their capacity to form dentin pulp–like tissue when transplanted into immunocompromised mice by using HA/TCP as a carrier (20–22). Therefore, DPSCs are considered to be suitable cells to evaluate odontogenic differentiation both *in vitro* and *in vivo*.

This is the first study to show that statin induces odontoblastic differentiation of DPSCs *in vitro* and *in vivo* (Figs. 3 and 4). The ability of statin to accelerate mineralized tissue formation *in vivo* was

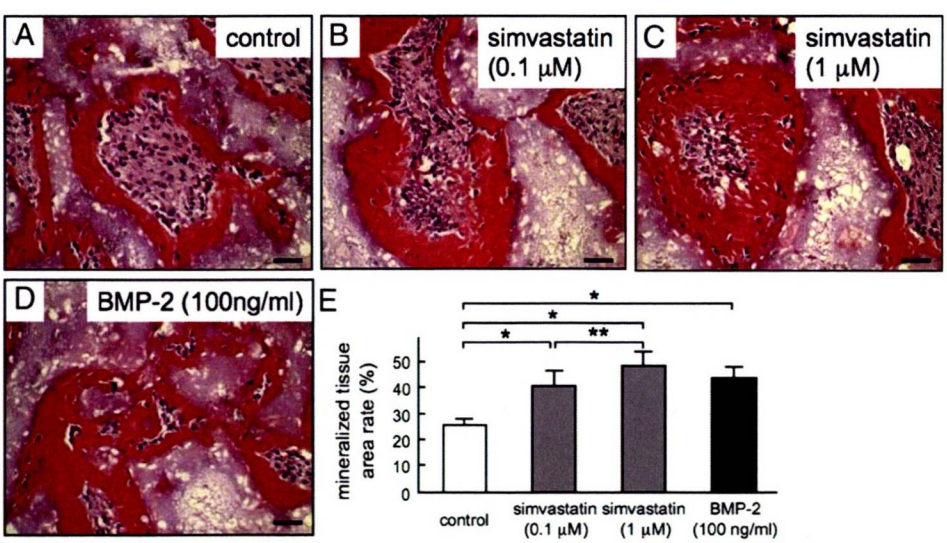

Figure 4. Simvastatin accelerated DPSC-mediated mineralized tissue formation *in vivo*. (*A–D*) All groups, including the control, showed mineralized tissue formation 8 weeks after transplantation. Importantly, mineralized tissue formed by simvastatin-treated cells formed tubular-like structures perpendicular to the surface of the carrier. Representative images are shown (scale bar, 100 μm). (*E*) DPSCs pretreated by simvastatin at 1 μmol/L or BMP-2 for 7 days formed significantly larger amount of mineralized tissue in comparison to the others (n = 4, one-way factorial ANOVA followed by Fisher PLDS tests: $*P < .0001$, $**P < .01$).

equivalent to BMP-2 (Fig. 4). Statin is known to accelerate BMP-2 expression and then enhance bone formation (18). However, our results showed the different effects of statin and BMP-2 on DPSCs in gene expression patterns (Fig. 3). Especially, statin significantly accelerated *dspp* gene expression in DPSCs. However, BMP-2 only slightly accelerated *dspp* gene expression, and the difference was not significant (Fig. 3*A*). The effect of BMP-2 on *dspp* gene expression observed in this study was inconsistent with a former report (29). The reason for this inconsistency might be due to the experimental conditions. In that report, a pellet culture was used, and the accelerated *dspp* gene expression was observed under BMP stimulation for more than 10 days (29). On the other hand, in this study, a monolayer culture was used, and the accelerated *dspp* gene expression was observed in a day-7 culture. In another report, an accelerated *dspp* gene expression was observed in a day-21 culture with the osteoinduction medium (containing dexamethasone, β-glycerophosphate, and ascorbic acid) (23). On the basis of these findings, statin might be a strong accelerator of *dspp* gene expression. Whether other pathways independent from BMP-2 stimulation could mediate the effects of statin on DPSCs, however, still needs further investigation.

The suppression of cell proliferation observed in this study (Fig. 1) is common to other cell types including osteoblastic cells, vascular smooth muscle cells, and neuronal cells (30–32). This suppression is mediated through the inhibition of the mevalonate and Rho pathways (25, 30, 32). Indeed, in DPSCs, mevalonate also effectively restored the proliferation suppressed by statin (Fig. 2*A*). Furthermore, statin inhibited actin fiber formation (Fig. 2*B*) and cell cycle progression (Fig. 2*C*) that is regulated by Rho. These results indicate that the suppression of proliferation in DPSCs is also mediated through the inhibition of the mevalonate and Rho pathways.

Pulp tissue contains a large amount of blood vessels and peripheral nerves. Statin is known to induce angiogenesis (13, 33) and to regulate the survival and increase neurogenesis of neuronal cells (34, 35), indicating the possible effectiveness of statin in pulp regeneration along with dentin regeneration. Furthermore, statin has an anti-inflammatory effect in various tissues. This could help restore the inflamed pulp tissue. Taken together, these results suggest that statin might be an ideal active ingredient in pulp capping material to accelerate reparative dentin formation. However, at the same time, attention has to be paid to the cell death observed in the cells treated with a high concentration of statin (Figs. 1 and 2*B*). This fact suggests that cells in pulp tissue might be damaged if statin acts on the cells at high concentration. Therefore, a careful evaluation is required before clinical application to determine the suitable concentration when applied indirectly to a cavity or directly to pulp tissue.

Acknowledgments

The authors thank Dr Eriko Aoyama (Biodental Research Center, Okayama University Dental School, Okayama, Japan) and Mr Yuya Yoshioka for the technical assistance. This work was supported in part by a Grant-in-Aid for Scientific Research (A) (No.17209062, to K.T.) from Japan Society for the Promotion of Science and a Grant-in-Aid for Young Scientists (A) (No.19689038, to W.S.) from the Ministry of Education, Culture, Sports, Science and Technology of Japan.

References

1. Salehrabi R, Rotstein I. Endodontic treatment outcomes in a large patient population in the USA: an epidemiological study. J Endod 2004;30:846–50.
2. Eckerbom M, Magnusson T, Martinsson T. Reasons for and incidence of tooth mortality in a Swedish population. Endod Dent Traumatol 1992;8:230–4.
3. Reuter JE, Brose MO. Failures in full crown retained dental bridges. Br Dent J 1984; 157:61–3.
4. Barthel CR, Rosenkranz B, Leuenberg A, Roulet JF. Pulp capping of carious exposures: treatment outcome after 5 and 10 years: a retrospective study. J Endod 2000; 26:525–8.
5. Casas MJ, Kenny DJ, Johnston DH, Judd PL. Long-term outcomes of primary molar ferric sulfate pulpotomy and root canal therapy. Pediatr Dent 2004;26:44–8.
6. Schroder U. Effects of calcium hydroxide-containing pulp-capping agents on pulp cell migration, proliferation, and differentiation. J Dent Res 1985;64(Spec No): 541–8.
7. Hu CC, Zhang C, Qian Q, Tatum NB. Reparative dentin formation in rat molars after direct pulp capping with growth factors. J Endod 1998;24:744–51.
8. Luisi SB, Barbachan JJ, Chies JA, Filho MS. Behavior of human dental pulp cells exposed to transforming growth factor-beta1 and acidic fibroblast growth factor in culture. J Endod 2007;33:833–5.
9. Lin ZM, Qin W, Zhang NH, Xiao L, Ling JQ. Adenovirus-mediated recombinant human bone morphogenetic protein-7 expression promotes differentiation of human dental pulp cells. J Endod 2007;33:930–5.
10. Nakashima M. Induction of dentine in amputated pulp of dogs by recombinant human bone morphogenetic proteins-2 and -4 with collagen matrix. Arch Oral Biol 1994;39:1085–9.
11. Rutherford B, Spangberg L, Tucker M, Charette M. Transdentinal stimulation of reparative dentine formation by osteogenic protein-1 in monkeys. Arch Oral Biol 1995;40:681–3.
12. Tziafas D, Alvanou A, Papadimitriou S, Gasic J, Komnenou A. Effects of recombinant basic fibroblast growth factor, insulin-like growth factor-II and transforming growth factor-beta 1 on dog dental pulp cells in vivo. Arch Oral Biol 1998;43: 431–44.
13. Kwak B, Mulhaupt F, Myit S, Mach F. Statins as a newly recognized type of immunomodulator. Nat Med 2000;6:1399–402.
14. Murohara T, Witzenbichler B, Spyridopoulos I, et al. Role of endothelial nitric oxide synthase in endothelial cell migration. Arterioscler Thromb Vasc Biol 1999;19: 1156–61.
15. van Nieuw Amerongen GP, Vermeer MA, Negre-Aminou P, Lankelma J, Emeis JJ, van Hinsbergh VW. Simvastatin improves disturbed endothelial barrier function. Circulation 2000;102:2803–9.
16. Yokoyama T, Miyauchi K, Kurata T, Satoh H, Daida H. Inhibitory efficacy of pitavastatin on the early inflammatory response and neointimal thickening in a porcine coronary after stenting. Atherosclerosis 2004;174:253–9.
17. Ayukawa Y, Yasukawa E, Moriyama Y, et al. Local application of statin promotes bone repair through the suppression of osteoclasts and the enhancement of osteoblasts at bone-healing sites in rats. Oral Surg Oral Med Oral Pathol Oral Radiol Endod 2008. Epub Sep 16, 2008.
18. Mundy G, Garrett R, Harris S, et al. Stimulation of bone formation in vitro and in rodents by statins. Science 1999;286:1946–9.
19. Kaji H, Naito J, Inoue Y, Sowa H, Sugimoto T, Chihara K. Statin suppresses apoptosis in osteoblastic cells: role of transforming growth factor-beta-Smad3 pathway. Horm Metab Res 2008;40:746–51.
20. Gronthos S, Brahim J, Li W, et al. Stem cell properties of human dental pulp stem cells. J Dent Res 2002;81:531–5.
21. Gronthos S, Mankani M, Brahim J, Robey PG, Shi S. Postnatal human dental pulp stem cells (DPSCs) in vitro and in vivo. Proc Natl Acad Sci U S A 2000;97: 13625–30.
22. Shi S, Robey PG, Gronthos S. Comparison of human dental pulp and bone marrow stromal stem cells by cDNA microarray analysis. Bone 2001;29:532–9.
23. Wei X, Ling J, Wu L, Liu L, Xiao Y. Expression of mineralization markers in dental pulp cells. J Endod 2007;33:703–8.
24. Ono M, Kubota S, Fujisawa T, et al. Promotion of attachment of human bone marrow stromal cells by CCN2. Biochem Biophys Res Commun 2007;357:20–5.
25. Hirai A, Nakamura S, Noguchi Y, et al. Geranylgeranylated rho small GTPase(s) are essential for the degradation of p27Kip1 and facilitate the progression from G1 to S phase in growth-stimulated rat FRTL-5 cells. J Biol Chem 1997;272:13–6.
26. Min KS, Lee HJ, Kim SH, et al. Hydrogen peroxide induces heme oxygenase1 and dentin sialophosphoprotein mRNA in human pulp cells. J Endod 2008;34:983–9.
27. Sonoyama W, Liu Y, Fang D, et al. Mesenchymal stem cell-mediated functional tooth regeneration in swine. PLoS ONE 2006;1:e79.
28. Shi S, Gronthos S. Perivascular niche of postnatal mesenchymal stem cells in human bone marrow and dental pulp. J Bone Miner Res 2003;18:696–704.
29. Iohara K, Nakashima M, Ito M, Ishikawa M, Nakasima A, Akamine A. Dentin regeneration by dental pulp stem cell therapy with recombinant human bone morphogenetic protein 2. J Dent Res 2004;83:590–5.
30. Tanaka T, Tatsuno I, Uchida D, et al. Geranylgeranyl-pyrophosphate, an isoprenoid of mevalonate cascade, is a critical compound for rat primary cultured cortical neurons to protect the cell death induced by 3-hydroxy-3-methylglutaryl-CoA reductase inhibition. J Neurosci 2000;20:2852–9.

31. Terano T, Shiina T, Noguchi Y, et al. Geranylgeranylpyrophosphate plays a key role for the G1 to S transition in vascular smooth muscle cells. J Atheroscler Thromb 1998;5:1–6.
32. Baek KH, Lee WY, Oh KW, et al. The effect of simvastatin on the proliferation and differentiation of human bone marrow stromal cells. J Korean Med Sci 2005;20:438–44.
33. Dimmeler S, Zeiher AM. Akt takes center stage in angiogenesis signaling. Circ Res 2000;86:4–5.
34. Lu D, Qu C, Goussev A, et al. Statins increase neurogenesis in the dentate gyrus, reduce delayed neuronal death in the hippocampal CA3 region, and improve spatial learning in rat after traumatic brain injury. J Neurotrauma 2007;24: 1132–46.
35. Miron VE, Rajasekharan S, Jarjour AA, Zamvil SS, Kennedy TE, Antel JP. Simvastatin regulates oligodendroglial process dynamics and survival. Glia 2007;55: 130–43.

Journal of Oral Rehabilitation 2009 **36**; 362–367

Polyphosphoric acid treatment promotes bone regeneration around titanium implants

K. MAEKAWA*, K. SHIMONO*, M. OSHIMA*, Y. YOSHIDA†, B. VAN MEERBEEK‡, K. SUZUKI† & T. KUBOKI* **Departments of Oral Rehabilitation and Regenerative Medicine, †Biomaterials, Dentistry and Pharmaceutical Sciences, Okayama University Graduate School of Medicine, Okayama, Japan and ‡Leuven BIOMAT Research Cluster, Department of Conservative Dentistry, School of Dentistry, Oral Pathology and Maxillo-Facial Surgery, Catholic University of Leuven, Leuven, Belgium*

SUMMARY **This study was conducted to evaluate the effect of polyphosphoric acid (PPA) treatment on bone regeneration around titanium (Ti) implants *in vivo*. Adsorption of PPA by Ti was achieved by immersing Ti implants (2 mm in diameter, 4 mm in length) in different concentrations of PPA solution (0, 1 and 10 wt%) for 24 h at 37 °C after proper Ti surface cleaning. The treated Ti implants were implanted on 8-week-old-male rat (n = 30) tibiae. Two or four weeks after implantation, all animals were deeply anaesthetized and underwent perfusion fixation. Ten specimens in each condition were further immersed in the same fixative for 1 week and eventually embedded in polyester resin. Afterwards, undecalcified sections were ground to a thickness of approximately 70 μm parallel to the long axis of the implant. The sections were stained with basic fuchsine and methylene blue and then examined by light microscopy. For quantitative evaluation of bone regeneration around the implants, the bone-implant contact ratio (BICR) was determined. Polyphosphoric acid treatment of the Ti implant surface significantly enhanced direct bone contact to the Ti surface. Especially, the BICRs of the 1 wt% PPA-treated Ti implants were significantly higher than those of the control untreated Ti implants, both 2 and 4 weeks after implantation. At 4 weeks, 10 wt% PPA-treated implants also significantly increased the BICR as compared to that of the untreated Ti implants. These results suggest that PPA treatment promotes osteoconductivity of Ti *in vivo*.**

KEYWORDS: **implant, titanium, polyphosphoric acid, bone formation, rat**

Accepted for publication 26 October 2008

Introduction

It is well known that the surface structure of the implant material that interfaces with bone plays an important role in osseointegration (1). Therefore, much *in vitro* and *in vivo* research is devoted to surface modifications of titanium (Ti) as well as to their biocompatibility with bone cells. Titanium surface modifications experimented include mechanical and/or chemical alterations of surface hydrophilicity, roughness, texture and morphology (2–6). In addition to such modifications, recent research interest has gradually shifted towards biological modification of implant surfaces by using e.g. cell growth factors, cell attachment factors and Arg-Gly-Asp peptides (7–10). Many bioactive surface coatings have been developed in an attempt to promote early osseointegration and bone formation around implants.

While such surface coatings have been shown to be effective with varying success, most of these procedures are rather complicated and/or costly for clinical use; virtually, none of them have currently been accepted as routine treatments to bioactivate implant surfaces. In this respect, a recent study has provided evidence that inorganic polyphosphate enhances human fibroblast proliferation as well as it promotes the mitogenic

doi: 10.1111/j.1365-2842.2008.01928.x